University of Khenchela-ABBES LAGHROUR
Faculty of Sciences and Technology
Industrial Engineering Department
جامـــعة عبـــاس لـــغرور خـنـشـلة
كليـــة العلـــوم والتكنـــولـــوجيـا
قسـم الهنـدسة الصنـاعية

Serial N°: .....

Final Year Project Report Presented in Partial Fulfilment of the Requirements for the Degree of

Master

In **Telecommunication**

Specialty : Telecommunications Systems

Title:

Broadband superconducting microstrip antennas on isotropic/anisotropic substrates

Presented by: - Miss. DJEBBAR Farah
- Miss. SLIMANI Kaouther

Before the jury composed of:

Dr. DOUAK Fouzi	***Chairman***	***University of Khenchela***
Pr. BEDRA Sami	***Advisor***	***University of Khenchela***
Dr. KHALFAOUI Fatima	***Examiner***	***University of Khenchela***

Jun 2022

ACKNOWLEDGMENTS

First of all, we thank the good ***GOD*** for having given us health and courage to carry out this work.

We would like to express our deep gratitude to our Promoter ***Pr: Sami Bedra***, for having us supervised and guided and for his invaluable help, his advice throughout our work.

We warmly thank the members of ***the jury:***

- ***Dr: Douak Fouzi***
- ***Dr: Khalfaoui Fatima***

For the honor they do us by agreeing to judge our graduation dissertation.

Our sincere feelings go out to ***our parents*** who sacrificed until today and for their encouragement all along our journey.

DEDICATION

We dedicate this modest work:

To our very ***dear parents***, may God protect them: ***our mother***, who is the light of our house, ***our father***, which is the guide to success in our life, for their help and their support throughout our studies, and we hope that: one day we will be able to give back a minimum of what they gave we.

To our ***dear brothers*** and our ***dear sisters***;

To all our friends; And finally, for everyone who knows we from near or far.

Farah & Kaouther

Table of Contents

Table of Contents

Chapter II

Mathematical Formulations

Chapter III

Superconducting Materials

Chapter IV

Numerical Results and Discussions

List of Figures and Tables

List of Figures

List of tables

General Introduction

General Introduction

The microstrip antenna (MSA), also called the patch antenna, was a new design structure patented in 1955. It did not find many applications in the first couple of decades; however, for the last few years, these have been widely used in wireless communication. In a microstrip antenna, dielectric material called substrate is sandwiched between two plates of the conducting materials [1]. The lower conducting surface and the upper conducting plate are called the ground plane and a patch, respectively. The patch and ground plane of the antenna are linked to the supply byline called the microstrip feed line. Many types of feeding methods are used to provide the supply to the antenna. The microstrip antennas are also known as the printed antennas because of the similar fabrication process of printed circuit board (PCB). These are very small-sized planar antennas that are very useful in wireless communication [2]. Installation of these antennas is very easy due to the fact that they are compact and lightweight. The size and shape of the patch are important aspects on which the performance of the microstrip antenna depends. Various shapes of the patch are being used to design the MSA [3].

Printed antennas are used in most classical microwave applications, including radars, telecommunications, wireless communication, satellites communication, mobile communications, aeronautical applications, the space industry, Global Positioning System (GPS), systems for detection and identification, and medical applications. In commercial sectors and industries, printed antenna uses include e-textiles, interactive point-of-sale displays, electronic toll collection, smart cards, and product packaging and equipment identification and tracking [4]. However, there are various techniques and design methodologies to make printed antennas behave differently and work in broadband applications.

High temperature superconducting (HTS) materials have been widely used in the manufacturing of diverse microwave devices for mobile. satellite and space communication [5]. The use of superconductive materials is expected to increase rapidly due to their low loss property at temperatures below the critical temperature (Tc). Also, they have the largest power gap size arrangement which extends their response well in the THz range [5]. The superconducting antenna is one of the first microwave components presented as an application

of a high-temperature superconductive material [5]. The main advantage of using superconductive materials in antenna systems is to reduce the loss associated with the adaptation lines of the transmission circuits and the power supply networks. in particular, at the microwave and millimeter frequencies where the ohmic losses begin to significantly affect system performance [5]. Thereby, HTS materials are often used in the manufacture of antennas to increase radiation efficiency and gain. Due to the low surface resistance in HTS thin films compared to copper and gold. However, high-temperature superconducting antennas like other conventional microstrip antennas suffer from narrow bandwidth, which severely limits their application [5].

Several methods are proposed to analyze microstrip antennas and can be classified into two groups: The first group gathers the methods simple intuitive. The second group contains rigorous analytical methods. The methods that we have just exposed are not the only theoretical means to predict the characteristics of microstrip antennas. Several electromagnetic (EM) simulation software for designing and simulating high-frequency electronic products such as HFSS (High Frequency Structure Simulator). However, it is more complex, allows less physical interpretation, and requires considerable computation time and memory space. Unlike low-frequency components, it is very difficult to adjust the characteristics of microstrip resonators once they are made. Therefore, it is necessary to have tools for the estimation of their characteristics, the best tool is CAD (Computing Aided Design). The real challenge in CAD lies in reliable numerical methods that offer both exact characteristics and reduced computation time [6].

Moreover, a lot of materials in current use as substrates exhibit a dielectric anisotropy (especially of the uniaxial type). Therefore, there is definitely a need to rigorously investigate the characteristics of microstrip antennas with anisotropic substrates. One of the well-established tools for the analysis more thoroughly of resonant characteristics of microstrip antennas on anisotropic substrates is the cavity model analysis.

Our work has twofold essential goals, the first one is to present the principles of soft computing techniques and their applications in the modeling of microstrip antennas printed on anisotropic substrates, and the second is to propose new design structures of HTS tapered microstrip antennas printed on anisotropic substrates. To make the work clear and comprehensible, our work is structured into four chapters covering different aspects of microstrip antennas.

The first chapter presents the microstrip antenna configuration and discusses its advantages, disadvantages, and applications. In addition, Chapter 1 briefly describes various theoretical methods for the analysis of microstrip antennas.

In chapter 2, an efficient approach based on the use of the cavity model in conjunction with electromagnetic knowledge is provided. This approach is used to characterize the tapered microstrip patch printed on anisotropic substrates.

Chapter 3 provides a survey on the theoretical behavior of superconducting materials since their discovery and their application in microwave engineering.

In the last chapter, we presented our numerical results of rectangular microstrip antenna printed on anisotropic substrates, as well as the results of the tapered substrates. The influence of the physical and geometrical parameters of the HTS antennas is presented.

Finally, we give a general conclusion of this work listing the different important phases of this manuscript. We will also give an overview of perspectives that can be developed to better understand this subject and also can be used in our future research.

References

[1] T.Karim and S.M .seddik, ‘’Modèle de cavité amélioré d’un résonateur microbande réglable pour l’application dans un équipement portable sans fil,’’ mémoire de master, université de khenchela , 2021.

[2] P. K. Malik, S. Padmanaban, and J. B. Holm-Nielsen, "*Microstrip Antenna Design for Wireless Applications*". CRC Press, 2021.

[3] A. Mahamdi, S. Benkouda, S. Aris, and T. A. Denidni, "Resonant Frequency and Bandwidth of Superconducting Microstrip Antenna Fed through a Slot Cut into the Ground Plane," *Electronics*, vol. 10, no. 2, p. 147, 2021.

[4] A. Pandey, "*Practical microstrip and printed antenna design*". Artech House, 2019.

[5] S. Bedra, S. Benkouda, R. Bedra, and T. Fortaki, "Inverted HTS rectangular patch antennas: Theoretical investigation," *Physica C: Superconductivity and its Applications*, vol. 580, p. 1353802, 2021.

[6] S. Bedra, R. Bedra, S. Benkouda, and T. Fortaki, "Efficient CAD Model to Analysis of High Tc Superconducting Circular Microstrip Antenna on Anisotropic Substrates," *Advanced Electromagnetics*, vol. 6, no. 2, pp. 40-45, 2017.

Chapter I

Overview of Microstrip Antennas

I.1. Introduction

The idea of microstrip patch antennas arose from utilizing printed circuit technology not only for the circuit components and transmission lines but also for the radiating elements of an electronic system. It was first proposed by Deschamps the concept of the microstrip antennas (MSAs) in 1953 [1]. However, practical antennas were developed by Munson [2]-[3] and Howell [4] in the 1970s.

The numerous advantages of microstrip antennas, such as their low weight, small volume, and ease of fabrication using printed-circuit technology, led to the design of several configurations for various applications [5]– [9]. With increasing requirements for personal and mobile communications, the demand for smaller and low-profile antennas has brought microstrip antennas to the forefront [10]. This first chapter aims to present the main concepts in this thesis, for this we have given an overview of the appearance and configuration of microstrip antennas, their mechanism of radiation, as well as the different feeding techniques Thus we also present the different types of power supply for patch antennas. We exhibit also the most common methods of analysis. Finally, we will end this chapter by presenting their applications, as well as their advantages and disadvantages.

I.2. Microstrip Antenna Description

Microstrip antennas also called “patch antennas”, One of the most useful antennas at microwave frequencies (f> 1 GHz) [11].

An MSA is a type of printed antenna, in its simplest form, consists of a radiating element(Patch), where the radiating Patch is a conductor attached directly to a microstrip feed line, usually made with copper on one side of a dielectric substrate and a ground plane on the other side, shown in Figure I.1.The radiation from the MSA can occur from the fringing fields between the periphery of the patch and the ground plane [10].

The dielectric substrates generally have a low permittivity ($\varepsilon_r \leq 3$) for facilitating and favoring the radiation, avoiding the confinement of the fields in the cavity between the radiating element and the ground plane.

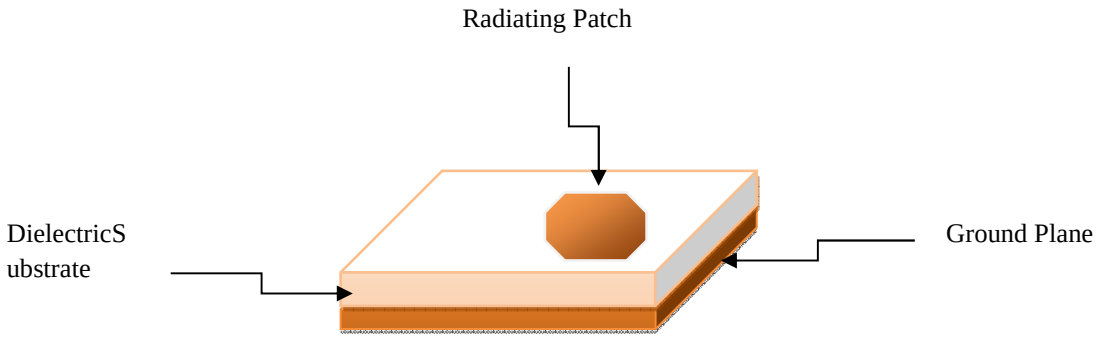

Figure I.1. Description of a microstrip antenna.

The patch may be in a variety shapes, such as the square, circular, triangular, rectangular, and elliptical…etc, shown in Figure I.2,Are also used, but rectangular and circular are the most common [10].

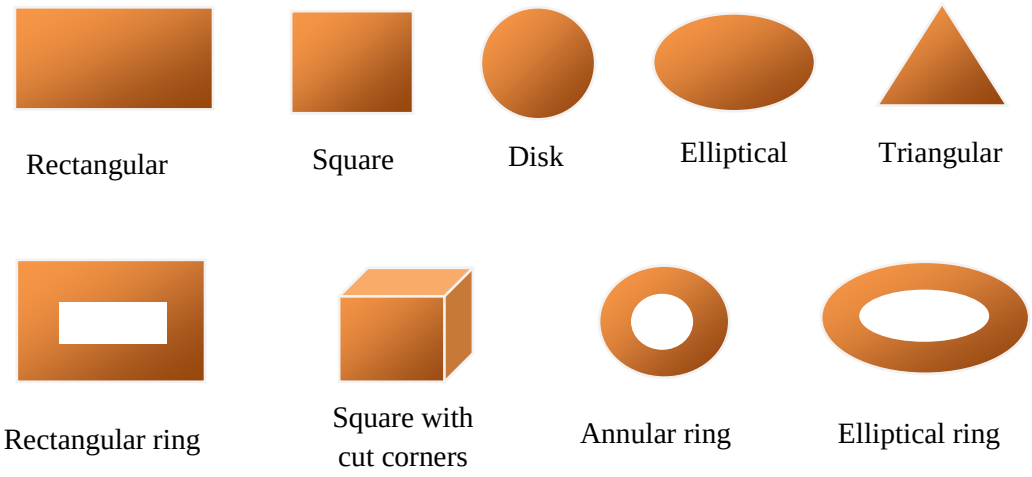

Figure I.2. Different shapes of microstrip patches.

The shapes of the radiating elements are shown in Figure I.2; their dimensions are generally of the order of $\lambda/2$ /2 to λ.

I.3. Material Consideration

The substrate material provides mechanical support for the radiating patch elements where the metallic patch is normally made of thin copper foil. It also maintains the required

spacing between the patch and its ground plane. The substrate thickness for the basic geometry is in the range of 0.01 to 0.05 free-space wavelength.

The dielectric constant ranges from 1 to 12 and can be separated into three categories:

- Those having a relative dielectric constant (relative permittivity) in the range of 1.0 to 2.0. This type of material can be air, polystyrene foam, or dielectric honeycomb;
- Those having a relative dielectric constant in the range of 2.0 to 4.0. This type of material consists mostly of Fiber-glass reinforced Teflon;
- Those with a relative dielectric constant between 4.0 and 10.0. This type of material can be ceramic, quartz, or alumina.

The most commonly used material is Teflon-based with a relative permittivity between 2 and 3. This material is also called PTFE (Poly Tetra Fluor Ethylene). It has a structure very similar to fiberglass material used for digital circuit boards but has a much lower loss tangent.

I.4. Basic Microstrip Antennas configurations

For the configuration of a microstrip patch antenna, we have to select the resonant frequency and a dielectric medium for which the antenna is to be designed. The parameters to be calculated are as under:

- Width (*W*): The width of the patch is calculated using the following equation [12], [13].

$$W = \frac{C_0}{2 f_r} \cdot \sqrt{\frac{2}{\varepsilon_r + 1}} \tag{I.1}$$

Where;

W : Width of the patch.

C_0 : Speed of light.

ε_r : Relative permittivity (dielectric constant) of the substrate.

- Effective refractive index: The effective refractive index value of a patch is an important parameter in the designing procedure of a microstrip patch antenna.

The radiations traveling from the patch towards the ground pass through the air and some through the substrate (called fringing). The value of the effective dielectric constant (ε_r) is calculated using the following equation [12], [13]:

$$\varepsilon_{reff} = \frac{\varepsilon_r + 1}{2} + \frac{\varepsilon_r - 1}{2} \cdot \left[1 + 12 \cdot \frac{W}{h}\right]^{-\frac{1}{2}} \quad \text{(I.2)}$$

- Length: Due to fringing, electrically the size of the antenna is increased by an amount of (ΔL). Therefore, the actual increase in length (ΔL) of the patch is to be calculated using the following equation [12], [13]:

$$\frac{\Delta L}{h} = 0.412 \cdot \frac{\left(\varepsilon_{reff} + 0.3\right) \cdot \left(\frac{W}{h} + 0.264\right)}{\left(\varepsilon_{reff} - 0.258\right) \cdot \left(\frac{W}{h} + 0.8\right)} \quad \text{(I.3)}$$

Where;

h: height of the substrate.

- The length (L) of the patch is now to be calculated using the below mentioned equation [12], [13]:

$$L = \frac{C_0}{2 f_r \cdot \sqrt{\varepsilon_r}} \cdot -2\Delta L \quad \text{(I.4)}$$

- Length (L_g) and width (W_g) of ground plane: Now the dimensions of a patch are known. The length and width of a substrate is equal to that of the ground plane. The length of a ground plane (L_g) and the width of a ground plane (W_g) are calculated using the following equations [14]:

$$L_g = L + 6h \quad \text{(I.5)}$$

$$W_g = W + 6h \quad \text{(I.6)}$$

The Figure I.3 below, shows the detailed configuration of the microstrip antenna.

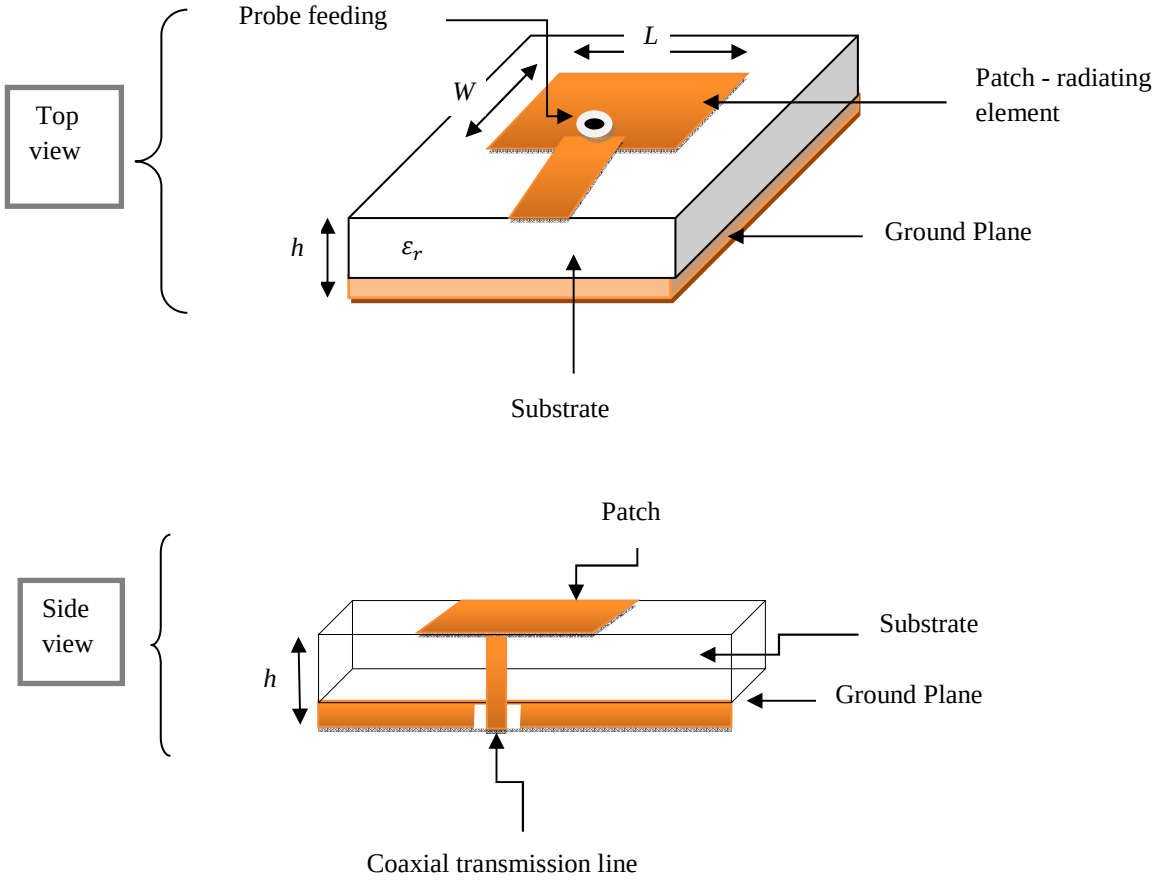

Figure I.3. Microstrip antenna configuration.

I.5. Radiation Mechanism of MSAs

The geometry of the microstrip antenna allows us to better understand its radiation mechanism. After the power supply line is excited by a radiofrequency source (RF), an electromagnetic wave propagates over the latter to meet the radiating element, which is generally wider than the line, in this case, we have a load distribution it will be created above and below the radioactive component and between ground level and the substrate. Figure I.4 illustrates this phenomenon. These distributions together with the correlation of the current densities generate a distribution of electric fields represented in Figure I.5.

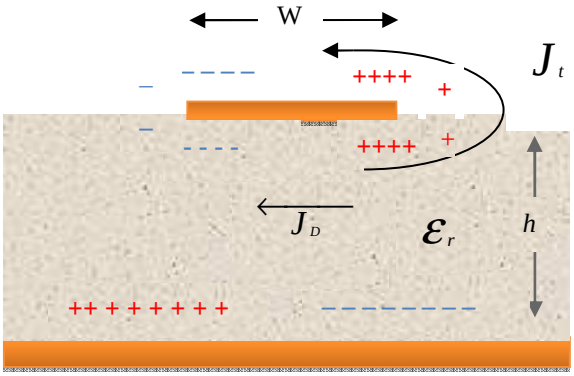

Figure I.4. Distribution charge and current density.

Its distribution extends around and inside the structure and is mainly dependent: the width W metallization circuits, the characteristics of the substrate: constant dielectric and its thickness h [15], [16].

With; J_D : Displacement current, and J_t: Surface current.

which will cause an inversion of the phases of the vertical components of the electric field along the length of the antenna and unlike the previous radiation which is in phase in the plane of the antenna is due to the components horizontal field lines surrounding the radiating element[17].

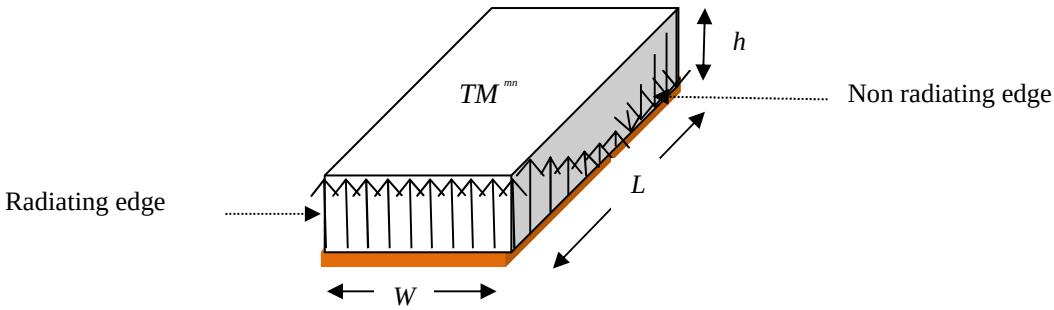

Figure I.5. Distribution of the vertical electric field.

The length L of the rectangular patch for the fundamental TM^{10} mode excitation is slightly smaller than $\lambda/2$, where λ is the wavelength in the dielectric medium, which in terms of

free-space wavelength λ_0 is given as $\lambda_0/\sqrt{\varepsilon_{reff}}$, where ε_{reff} is the effective dielectric constant of a microstrip line of width W .

To better understand the radiation mechanism of microstrip antennas, the scientific literature is generally based on the theory of optics. Consider the cut given in Figure I.6.

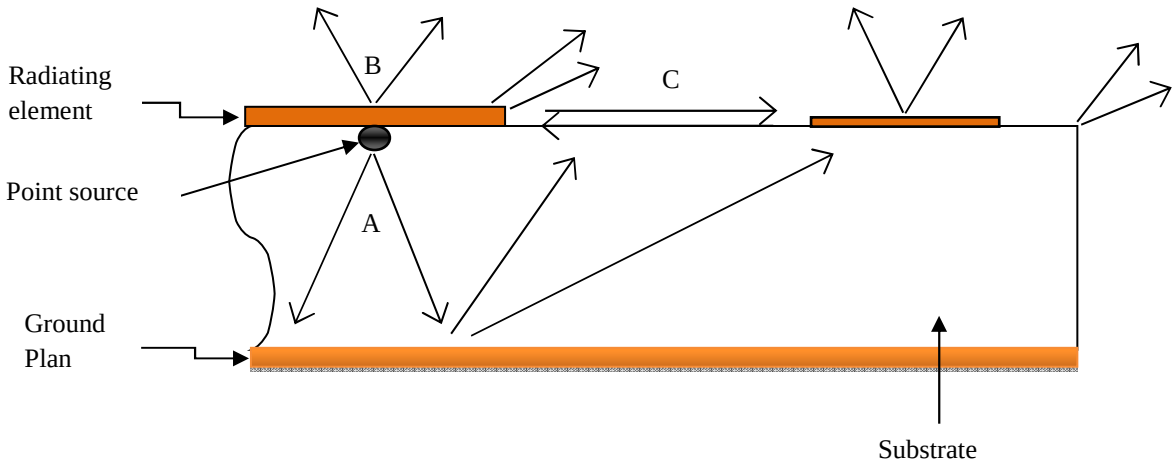

Figure I.6. Radiation in a microstrip antenna.

At point (A) of the upper conductor, a point source (surface current density) has been deposited, which radiates in all directions. Part of the transmitted signal is reflected by the ground plane, then by the upper conductor and so on. Some of these rays end on the edge of the conductor, which diffracts them and consequently the field breaks up into two components normal and tangential with respect to the ground plane [18-20]. We can therefore consider three regions:

- Directed waves in region A: In the substrate, the rays are the most focused. Where the electromagnetic field accumulates in this region of space. This property is very useful for spreading the signal along the microstrip line;
- Radiated waves in region B: above the substrate (in the air), the signal disperses freely in space and contributes to the radiation of the antenna. As the surface currents circulate mainly on the underside of the upper conductor (dielectric side),the radiation seems especially to be emitted by the immediate vicinity of the edges;
- Surface waves in region C: Some rays reach the separating surfaces witha grazing incidence, and remain trapped inside the dielectric. This is the mechanism of total reflection, which optical fibers use. Where the surface wave is guided by the edge of

the dielectric, not contributing directly to the radiation of the antenna. However, when this wave reaches the edge of the substrate (point C), it is diffracted and generates stray radiation.

I.6. Feeding Techniques

The feeding technique depends in part on the final geometry and configuration desired from the antenna. Another important aspect to consider in feeding the antenna is the connection problem. The adaptation is always necessary between the network power supply and the antenna, as it ensures maximum power transfer to the load (antenna). In other words, the antenna input impedance should be as close as possible to the commonly used line impedance of 50 Ohms. Feeding technique influences the input impedance and characteristics of the antenna, and is an important design parameter.

The MSA can be excited into two main ways:

- Directly either by a coaxial probe or by a microstrip line;
- Indirectly using electromagnetic coupling or aperture coupling and a coplanar waveguide feed, in which case there is no direct metallic contact between the feed line and the patch.

I.6.1. The Direct Feed

I.6.1.1. Coaxial Probe

The coaxial or probe feed arrangement is shown in Figure I.7. The central (inner) conductor is soldered directly to the radiating element (patch) after passing through the dielectric and the ground plane, the outer conductor is connected directly to the latter. The main advantage of this feed is that it can be placed at any desired location insidethe patch to match with its input impedance. The disadvantages are thatthe hole has to be drilled in the substrate and that the connector protrudesoutside the bottom ground plane, so that it is not completely planar. Also,this feeding arrangement makes the configuration asymmetrical [21].

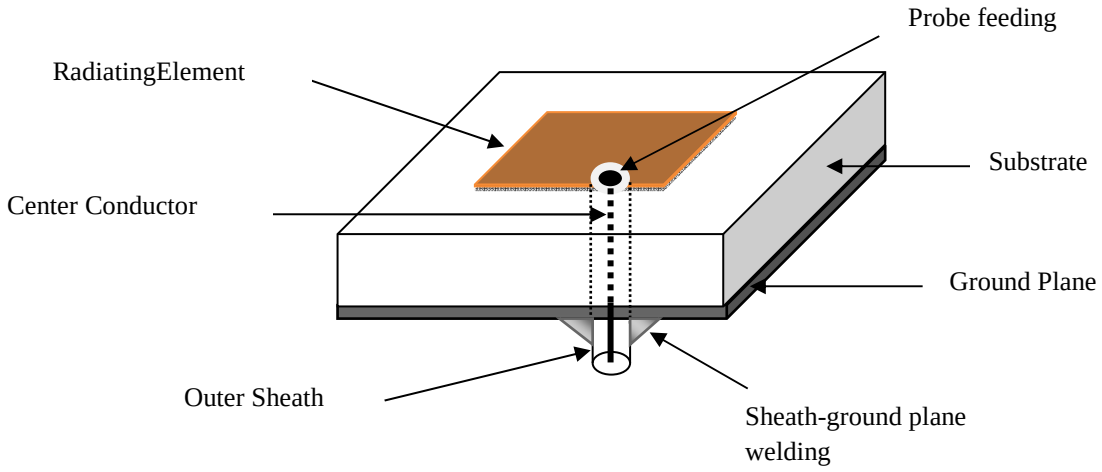

Figure I.7. Feeding by coaxial probe.

I.6.1.2. Microstrip-Line

In this feed, a microstrip line is connected directly to the edge of the patch is shown in Figure I.8, This line is smaller regarding the width compared to the patch [22].

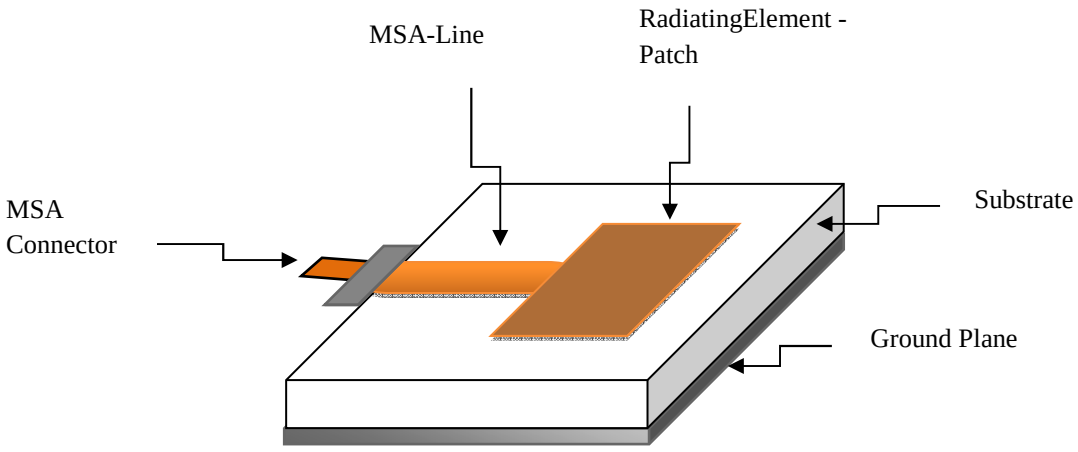

Figure I.8. Feeding by a microstrip line.

This technique feed can be supplied via:

- Direct connection with a microstrip line (usually 50 Ohms) whose point junction is on the axis of symmetry of the radiating element (Figure I.8);
- Offset from this axis of symmetry (A);

- Axial feed with a notch that allows for better adaptation of impedance (B).

A: Offset. B: Axial feed with a notch.

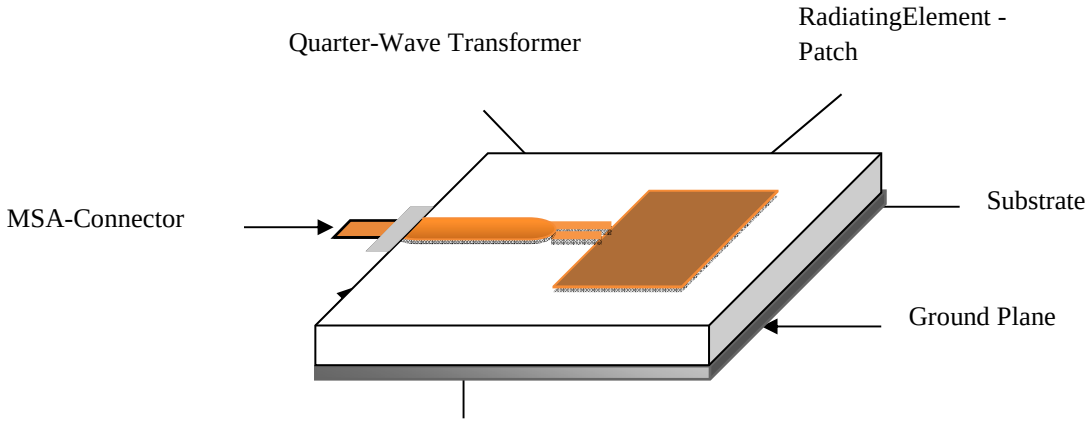

C: Quarter wave line.

Figure I.9. Different techniques of feeding by a microstrip line.

- Power supply (axial or offset) adapted by quarter wave line (C): At the edge of a patch, the impedance is generally much higher than 50 Ohms (e.g. 200 Ohms). To avoid impedance mismatch, sections of quarter-wavelength transformers can be used to transform large input impedance to a 50 Ohms line.

This feed arrangement has the advantage that it can be etched on the same substrate, so the total structure remains planar. The drawback is the radiation from the feed line, which leads to an increase in the cross-polar level. Also, in the millimeter-wave range, the size of the feed line is comparable to the patch size, leading to increased undesired radiation [10].

I.6.2. The Indirect Feed

Both the above methods of direct feeding the MSA have problems. In the case of a coaxial feed, increased probe length makes the input impedance more inductive, leading to the matching problem. For the microstrip feed, an increase in the substrate thickness increases its width, which in turn increases the undesired feed radiation. The indirect feed discussed below, solves these problems.

I.6.2.1. Electromagnetically coupled

The electromagnetic coupling is also known as proximity coupling, where the feed line is placed between the patch and the ground plane, which is separated by two dielectrics substrates:

- Antenna Substrate, which features the patch at the top;
- Feed Substrate, whose ground plane is engraved at the bottom.

The electromagnetic coupling is done independently and without contact of the line MSA supply with the patch, which minimizes parasitic radiation [23].

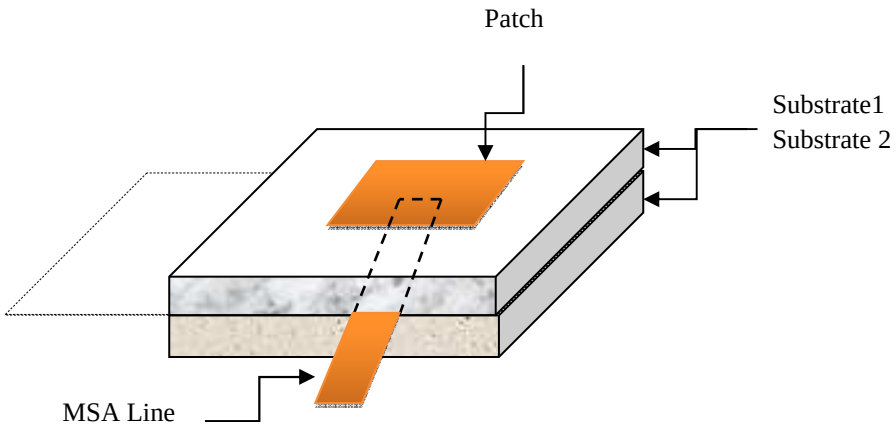

Figure I.10. Proximity coupled microstrip feed.

I.6.2.2. Aperture coupling

In the aperture-coupled MSA configuration, the field is coupled from the microstrip line feed to the radiating patch through an electrically small aperture or slot cut in the ground plane, as shown in Figure I.11. This aperture-coupling technique can be used to avoid

soldering connection as well as to avoid leakage radiation of the line to interfere with the patch radiation. In addition, by using a thick substrate, this feed method allows the patch to achieve a wider bandwidth (>10%) compared to the coaxial probe feed [24].

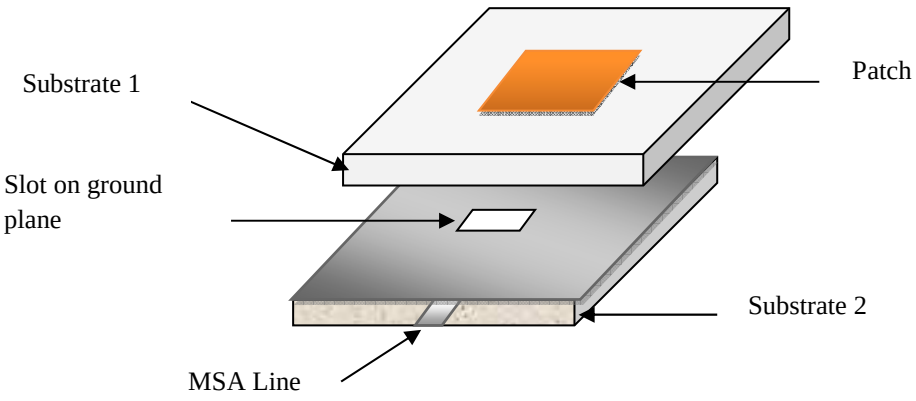

Figure I.11. Aperture coupled feed.

I.6.2.3. Coplanar Waveguide (CPW)

In this method of feed, the coplanar line and the ground plane are located on the same face shown in Figure I.12.

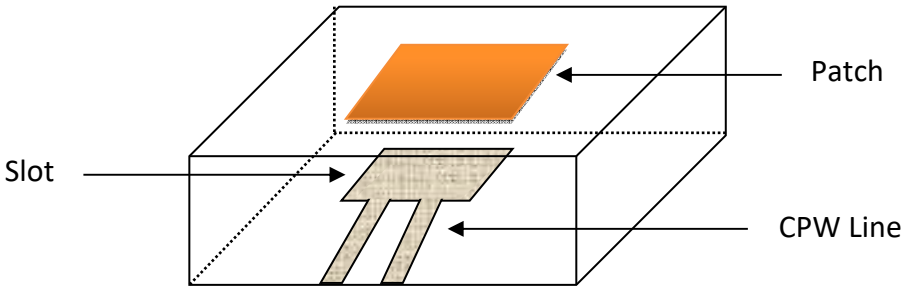

Figure I.12. The coplanar waveguide feed.

The line is excited by a coaxial feed and is terminated by a slot, whose length is chosen to be between 0.25 and 0.29 of the slot wavelength. The main disadvantage of this method is the high radiation from the rather longer slot, leading to the poor front-to-back ratio. The front-to-back ratio is improved by reducing the slot dimension and modifying its shape in the form of a loop [25].

An antenna fed by a coplanar waveguide CPW (Coplanar Wave Guide) is simpler than that powered by slot coupling.

I.6.3. Comparison between different feeding methods

Table 1. Comparison between different feeding methods.

Characteristics	coaxial feed	MSA Line feed	Aperture Coupled Feed	Proximity Coupled feed
Radiation parasite	More	More	Less	Minimum
Reliability	Poor	Better	Good	Good
Ease of manufacture	Soldering and drilling required	Easy	Alignment required	Alignment required
Bandwidth	2 à 5 %	2 à 5 %	2 à 5 %	15 %

I.7. Analysis Methods of MSAs

The MSA generally has a two-dimensional radiating patch on a thin dielectric substrate and therefore may be categorized as a two-dimensional planar component for analysis purposes, is a relatively complicated radiator. Over the years there have been several analytical/numerical methods proposed and used to analyze this radiator [26], where these methods can be grouped as either approximate techniques or full-wave analyses. The approximate techniques, the transmission line model and the cavity model use simplifying assumptions to reduce the complexity of the analysis of the antenna.The analysis methods for MSAs can be broadly divided into two groups:

In the first group, there are three popular analytical techniques based on equivalent magnetic current distribution around the patch edges (similar to slot antennas):

I.7.1. Transmission line model

The earliest useful model introduced to provide approximate values of resistance at the edge of a microstrip antenna is known as the transmission line model, introduced by Munson, is the easiest way to study the microstrip antenna. In this method the transmission line model represents the microstrip patch antenna by two radiating slots (apertures), each of width W and height h and separated by a low-impedance transmission line of length L. Results we get

are not the best accurate compared with other methods but it is good enough to design the antenna. To study the theory of microstrip transmission line we have two different cases:

- $\frac{W}{h} < 1$ (narrow strip line) and this is not what we are interesting with;
- $\frac{W}{h} >> 1$ and $\varepsilon_r > 1$ (wider transmission line) this will help us to build a good representation to study the antenna.

This model was originally developed for rectangular patches but has been extended for generalized patch shapes, where many variations of this method have been used to analyze the MSAs. Although the transmission line model is easy to use, all types of configurations cannot be analyzed using this model since it does not take care of variation of field in the orthogonal direction to the direction of propagation[27]-[29].

I.7.2. Cavity model

The cavity model originated in the late 1970s, is more dependable than the transmission line model, where in analyzing the microstrip antennas is based on the assumption that the region between the patch and the ground plane is treated as a cavity that is surrounded by magnetic walls around the periphery and by electric walls from the top (in $z = h$, the upper metallic conductor), and bottom sides (in $z = 0$, ground plane). Since thin substrates are used, the field inside the cavity is uniform along the thickness of the substrate [10]. This method makes it possible to determine in an approximate way the resonant frequency f^{mn} and the effective permittivity in the case of a rectangular radiating element of dimension (L, W).

The cavity model does handle non-contact feed patch solutions (such as an aperture coupled patch) more accurately than it does for a direct contact (for example probe fed) fed patch. This can be attributed to lack of a current discontinuity for non-contact fed patch antennas, which the cavity model has difficulty is predicting the associated modes [26].

These techniques (Transmission Line and the Cavity models) can be relatively accurate. When one such condition is that the substrate is relatively thin (less than $0.02\lambda_0$). Another condition is that the dielectric constant be relatively low.

A distinct advantage of the approximate techniques is the speed in determining the predicted performance and hence the use of these methods for obtaining overall trends. However, if minimal iterations of a design are required and the performance goals are difficult for a conventional microstrip patch to meet, then the approximate techniques should not be relied upon.

In the second group, the methods are based on the electric current distribution on the patch conductor and the ground plane (similar to dipole antennas, used in conjunction with full-wave simulation/numerical analysis methods). Some of the numerical methods for analyzing MSAs are listed as follows:

I.7.3. The Method of Moments (MM)

In the 1980s, the method of moments (MM) became the first numerical analysis method that was computationally efficient enough so that contemporary computers could provide enough memory and CPU speed to practically analyze microstrip antennas. In this technique advanced by Newman, the method of moment is used in connection with Richmond's reaction method to determine unknown surface currents flowing on the walls forming the microstrip patch, ground plane, and magnetic walls, and volume polarization currents in the dielectric slab are used to model the fields in the dielectric slab [30-31].

The integral equations are transformed into algebraic equations that can be easily solved using a computer. This method takes into account the fringing fields outside the physical boundary of the two-dimensional patch, thus providing a more exact solution.

I.7.4. The Finite-Element Method (FEM)

Improvements in computational power and memory size of personal computers during the 1990s made other numerical methods such as finite element method (FEM), which require much more memory than MM solutions, workable for everyday use by designers.

The FEM, unlike the MM, is suitable for volumetric configurations. In this method, the region of interest is divided into any number of finite surfaces or volume elements depending upon the planar or volumetric structures to be analyzed [32]. These discredited units, generally referred to as finite elements, can be any well-defined geometrical shapes such as triangular elements for planar configurations and tetrahedral and prismatic elements

for three-dimensional configurations, which are suitable even for curved geometry. It involves the integration of certain basic functions over the entire conducting patch, which is divided into a number of subsections. The problem of solving wave equations with inhomogeneous boundary conditions is tackled by decomposing it into two boundary value problems, one with Laplace's equation with an inhomogeneous boundary and the other corresponding to an inhomogeneous wave equation with a homogeneous boundary condition [33].

I.7.5. The Finite-Difference Time-Domain (FDTD)

The Finite-Difference Time-Domain method (FDTD) is today's one of the most popular technique for the solution of electromagnetic problems. It has been successfully applied to an extremely wide variety of problems, such as scattering from metal objects and dielectrics, antennas, microstrip circuits, and electromagnetic absorption in the human body exposed to radiation. The main reason of the success of the FDTD method resides in the fact that the method itself is extremely simple, even for programming a three-dimensional code. The technique was first proposed by K. Yee, and then improved by others in the early 70s.

In this technique, spatial as well as time grid for the electric and magnetic fields are generated over which the solution is required. The spatial discretization along three Cartesian coordinates are taken to be same. The E cell edges are aligned with the boundary of the configuration and H fields are assumed to be located at the center of each E cell. Each cell contains information about material characteristics. The cells containing the sources are excited with a suitable excitation function, which propagates along the structure [10].

I.7.6. The Spectral Domain Approach (SDA)

The method was originally developed by Itoh and Menzel in the early 1980s (references are given at the end). In the SDA, a two-dimensional Fourier transform along the two orthogonal directions of the patch in the plane of substrate is employed. Boundary conditions are applied in Fourier transform plane. The current distribution on the conducting patch is expanded in terms of chosen basis functions, and the resulting matrix equation is solved to evaluate the electric current distribution on the conducting patch and the equivalent magnetic current distribution on the surrounding substrate surface. The various parameters of the antennas are then evaluated [34].

I.8. Applications of MSAs

The microstrip patch antennas are being used in a large variety of applications, where a large number of commercial needs are met by the use of microstrip and printed antennas; these include the Global Positioning System (GPS), Zigbee, Bluetooth, WiMax, WiFi applications, and others.

- GPS applications: such as asset tracking of vehicles as well as marine uses, have created a large demand for antennas. The majority of these are rectangular patches that have been modified to produce right-hand circular polarization (RHCP) and operate at 1.575 GHz. Numerous vendors offer patches designed using ceramics with a high dielectric constant (ε_r = 6, 20, 36) to reduce the rectangular microstrip antenna to as small a footprint as possible for a given application. Rectangular patch antennas are also used for Bluetooth automotive applications (2.4 GHz) [31];
- SDARS: In recent years Satellite Digital Audio Radio Services (SDARS) have become a viable alternative to AM and FM commercial broadcasts in automobiles. The system has strict radiation pattern requirements which have been met with a combination of a printed monopole and a TM21 mode annular microstrip antenna that has been altered with notches to produce left-hand circular polarization at 2.338 GHz;
- WLAN (Wireless local area networks) provide short-range, high-speed data connections between mobile devices (such as a laptop computer) and wireless access points. The range for wireless data links is typically around 100 to 300 feet indoors and 2000 feet outdoors;
- Multiband printed antennas that are integrated into ceiling tiles use a microstrip diplexer to combine the signal from Global System for Mobile communication (GSM) cell phones (860 MHz band), personal communications services (PCS) cell phones (1.92 GHz band), and 802.11a WLAN service (2.4 GHz band) provided by two integrated microstrip dipoles. Wireless local area network systems sometimes require links between buildings that have wireless access points. This is sometimes accomplished using microstrip phased arrays at 5 GHz;
- Omni-directional microstrip antennas are also of utility for many WiMax applications (2.3, 2.5, 3.5, and 5.8 GHz are some of the frequencies currently of interest for WiMax applications) and for access points. Microstrip fed printed slot

antennas have proven useful to provide vertical polarization and integrate well into laptop computers for WLAN [31];

- Communication systems: The advantages of using antennas in communication systems will continue to generate new applications which require their use, which have the advantages of mobility without any required physical connection. The use of a transmission line, such as a coaxial cable or waveguide, may have an advantage in transmission loss for short lengths, but as distance increases, the transmission loss between antennas becomes less than any transmission line, and in some applications can outperform cables for shorter distances. The material costs for wired infrastructure also encourage the use of antennas in many modern communication systems [31].

Another application receiving attention is the utilization of patch antennas for biomedical telemetry services. Once again because of the small size and the ease of integration with microwave components, the microstrip patch is an obvious choice. Here because often the communicating sensor may be located within the skin of the user, the size of the antenna must be minimized. Fortuitously, such applications require relatively narrow bandwidths, compared to mobile communications systems [26].

I.9. Advantages and Disadvantages of Microstrip Antenna

The MSA has proved to be an excellent radiator for many applications because of its several advantages, but it also has some disadvantages.

I.9.1. Advantages

MSAs have several advantages compared to the conventional microwave antennas. The main advantages of MSAs are:

- Their ease of mass production using printed-circuit technology leads to a low fabrication cost (Low-cost fabrication);
- Can easily conform to a curved surface of a vehicle or product;
- Resistant to shock and vibration (most failures are at the feed probe solder joint);
- Many designs readily produce linear or circular polarization;
- Considerable range of gain and pattern options (2.5 to 10.0 dB);

- Other microwave devices realizable in microstrip may be integrated with a microstrip antenna with no extra fabrication steps (e.g., branch line hybrid to produce circular polarization or corporate feed network for an array of microstrip antennas);
- They are lightweight and have a small volume and a low-profile planar configuration, Antenna thickness (profile) is small;
- They can be made compact for use in personal mobile communication;
- They allow for dual- and triple-frequency operations.

I.9.2. Disadvantages

MSAs suffer from some disadvantages as compared to conventional microwave antennas. They are:

- Narrow bandwidth (5% to 10% [2:1 voltage standing wave ratio (VSWR)] is typical without special techniques);
- Dielectric and conductor losses can be large for thin patches, resulting in poor antenna efficiency;
- Sensitivity to environmental factors such as temperature and humidity;
- Lower gain;
- Low power-handling capability.

MSAs have narrow (BW), typically 1–5%, which is the major limiting factor for the widespread application of these antennas. Increasing the BW of MSAs has been the major thrust of research in this field, and broad BW up to 70% has been achieved [10], [31].

I.10. Conclusion

In this chapter, we have presented the different feeding techniques of microstrip antennas as well as the advantages and disadvantages of these types of antennas. In addition, we presented the analytical methods used to deal with this kind of antenna, we basing on the different electromagnetic models. Which should be enough to understand the general operation of planar antennas used in wireless communication systems.

The problem of bandwidth still remains a hindrance in communication systems, it is, therefore, necessary to modify the conventional structure of the microstrip antenna in order

to meet the increasingly increased requirements of the systems of modern communications. However, several techniques gain enhancements have been implemented to overcome this drawback, therefore will be our objective in the following chapters.

I.11. References

[1] Deschamps, G. A., ‘‘Microstrip Microwave Antennas,’’ Proc. 3rd USAF Symposium on Antennas, 1953.

[2] Munson, R. E., ‘‘Single Slot Cavity Antennas Assembly,’’ U.S. Patent No. 3713162, January 23, 1973.

[3] Munson, R. E., ‘‘Conformal Microstrip Antennas and Microstrip Phased Arrays,’’ IEEE Trans. Antennas Propagation, Vol. AP-22, 1974, pp. 74–78.

[4] Howell, J. Q., ‘‘Microstrip Antennas,’’ IEEE Trans. Antennas Propagation, Vol. AP-23, January 1975, pp. 90–93.

[5] Bahl, I. J., and P. Bhartia, Microstrip Antennas, Dedham, MA: Artech House, 1980.

[6] Carver, K. R., and J. W. Mink, ‘‘Microstrip Antenna Technology,’’ IEEE Trans. Antennas Propagation, Vol. AP-29, January 1981, pp. 2–24.

[7] Mailloux, R. J., et al., ‘‘Microstrip ArrayTechnology,’’ IEEE Trans. Antennas Propagation, Vol. AP-29, January 1981, pp. 25–37.

[8] James, J. R., et al., ‘‘Some Recent Development in Microstrip Antenna Design,’’ IEEE Trans. Antennas Propagation, Vol. AP-29, pp. 124–128, January 1981.

[9] James, J. R., and P. S. Hall, Handbook of Microstrip Antennas, Vol. 1, London: Peter Peregrinus Ltd., 1989.

[10] Girish Kumar, and K. P. Ray., ‘‘Broadband Microstrip Antennas,’’ India, October 2002.

[11] David R, and Jackson Dept., “Microstrip Antennas” of ECE University of Houston.July7-13, 2013.

[12] Ramna, Amandeep Singh Sappal.,“ Design of rectangular microstrip patch antenna using particle swarm optimization,” International Journal of Advanced Research in Computer and Communication EngineeringVol. 2, Issue 7, July 2013.

[13] MarufAhamed, Kishore Bhowmik, Abdulla Al Suman., “Analysis and Design of Rectangular Microstrip Patch Antenna on Different Resonant Frequencies for Pervasive Wireless Communication,” International journal of scientific & research , volume 1, issue 5, June 2012.

[14] Sukhbir Kumar, Hitender Gupta.,” Design and Study of Compact and Wideband Microstrip U-Slot Patch Antenna for Wi-Max Application,” IOSR Journal of Electronics and Communication Engineering (IOSR-JECE) e-ISSN: 2278-2834p- I. Volume 5, Issue 2 (Mar. - Apr. 2013), PP 45-48.

[15] ChorfiHamid., ”Conception d’un nouveau système d’antenne réseau conforme aux ondes millimétrique,” mémoire pour l’obtention Université de Quebec, Mai 2012.

[16] Vaudon Patrick., ”Les antennes cornets,”mémoire de maitrise en Télécommunication. IRCOM-Université de Limoges.

[17] Visser. J. H., ”Array and Phased Array Antenna Basics,” Antenna Engineer. The Netherlands 2005.

[18] Bedra Sami, "Evaluation analytique et numérique des caractéristiques électromagnétiques des structures microbandes ouvertes," Thèse doctorat e-sciences, Département d’électronique, université de Batna 2, Algérie, 2015.

[19] Benkouda Siham, "Contribution à l’étude des problèmes de caractérisation des antennes microrubans à plaques rayonnantes parfaitement conductrices et supraconductrices, " Thèse doctorat e-sciences, Département d’électronique, université de Batna, Algérie, 2012.

[20] Djelloul Aissaoui, "Analyse à l ’Aide de Modèles Equivalents d’Antennes Imprimées Alimentées par Lignes Adaptées, "Thèse de Magister en Electronique Signaux & Systèmes, université Abou BakrBelkaid -Tlemcen, Algérie, 2007.

[21] Balanis. C. A, "Antenna theory analysis and design," 2 edition John Wiley and Sons, 1997.

[22] AMEZIANE Djamel, "Etude et optimisation d’antennes fractales plaquées, "Magister télécom, 20 mai 2009.

[23] Chetouah. Farouk, " Etude et modélisation des antennes miniatures basées sur des matériaux diélectriques," Thèse doctorat en sciences, Département d’électronique, université Ferhat Abbas Sétif 1, Algérie, 2018.

[24] Pozar, D. M., "Microstrip Antenna Aperture-Coupled to a Microstrip Line," Electronics Letters, Vol. 21, No. 2, 1985, pp. 49–50.

[25] Smith, R. L., and J. T. Williams., "Coplanar Waveguide Feed for Microstrip Patch Antenna," Electronics Letters, Vol. 28, No. 25, 1992, pp. 2272–2274.

[26] Waterhouse, R.B. (Rodney B.),’’Microstrip patch antennas: a designer's guide’’ of RMIT University, 2003.

[27] Bhatacharya, A. K., and R. Garg., ‘‘Generalized Transmission Line Model for Microstrip Patches,’’ IEE Proc. Microwaves, Antennas Propagation, Pt. H, Vol. 132, No. 2, 1985, pp. 93–98.

[28] Dubost, G., and G. Beauquet. ‘‘Linear Transmission Line Model Analysis of a Circular Patch Antenna,’’ Electronics Letters, Vol. 22, October 1986, pp. 1174–1176.

[29] Babu, S., I. Singh, and G. Kumar., ‘‘Improved Linear Transmission Line Model for Rectangular, Circular and Triangular Microstrip Antennas,’’ IEEE AP-S Int. Symp. Digest, July 1997, pp. 614–617.

[30] David, M. Pozar., and Daniel, H., ‘’ The Analysis and Design of Microstrip Antennas and Arrays –wley-IEEE Press,’’ 1995.

[31] Bancroft and Randy, ‘’ Microstrip and Printed Antennas,’’

[32] Silvester, P., ‘‘Finite Element Analysis of Planar Microwave Network,’’ IEEE Trans. Microwave Theory Tech., Vol. MTT-21, 1973, pp. 104–108.

[33] Lee, H. F., and W. Chen, Advances in Microstrip and Printed Antennas, New York: John.

[34] Itoh, T., and W. Menzel, ‘‘A Full-Wave Analysis Method for Open Microstrip Structure,’’ IEEE Trans. Antennas Propagation, Vol. AP-29, January 1981, pp. 63–68.Wiley& Sons, 1997.

II. Introduction

The microstrip antennas have been widely used in recent years because of their good characteristics, where they can be printed directly onto a circuit board, they are electrically thin, lightweight and low cost, conformable and so on [1]. However, the electrical performance of the basic microstrip antenna suffers from a number of serious drawbacks, including very narrow bandwidth, high feed network losses, high cross polarization, and low power handling capacity. With progress in both theory and technology, some of these drawbacks have been overcome, or at least alleviated to some extent [2].

One method commonly used to model microstrip antennas is the Magnetic Cavity Model. The cavity model of the MSA assumes that the patch and the ground plane are electric walls, and the periphery of the patch is a magnetic wall. The fields in the resulting cavity are assumed to be the fields of the antenna and Huygens Principle is applied at the magnetic wall to determine radiation. To determine the fields within the cavity, a solution of an inhomogeneous wave equation is required. Therefore, the Magnetic Cavity Model is most easily applied when the method of separation of variables is applicable. The rectangular and circular patch MSAs are symmetric in two planes. Therefore, the cavity model is convenient in both cases. For arbitrarily shaped patches, application of the Method of Moments to the integral equation is necessary to avoid tedious calculations [3]. The magnetic cavity model works best for a thin substrate. The cavity model is generally accurate in its impedance prediction and is within 3% of measured resonant frequency for a substrate thickness of $0.02\lambda_0$ or less. In this chapter, we modify the cavity method developed later to the analysis of rectangular microstrip antennas, but the analytical study can also be for a tapered microstrip patch antenna.

II.2. Cavity Model Description

The cavity model, originated in the late 1970s by Lo et al, in the cavity model, the region between the patch and the ground plane is treated as a cavity that is surrounded by magnetic walls around the periphery and by electric walls from the top and bottom sides. Since thin substrates are used, the field inside the cavity is uniform along the thickness of the substrate. The fields underneath the patch for regular shapes such as rectangular, circular, triangular,

and sectoral shapes can be expressed as a summation of the various resonant modes of the two-dimensional resonator. The fringing fields around the periphery are taken care of by extending the patch boundary outward so that the effective dimensions are larger than the physical dimensions of the patch. The effect of the radiation from the antenna and the conductor loss are accounted for by adding these losses to the loss tangent of the dielectric substrate. The far field and radiated power are computed from the equivalent magnetic current around the periphery |4].

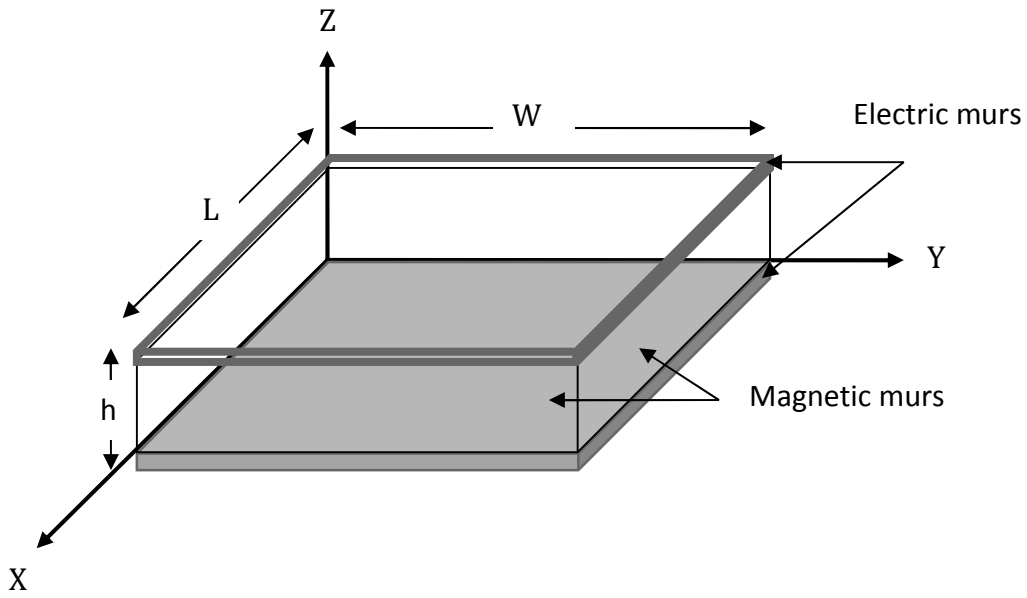

Figure II.1. The cavity model.

Although the transmission line model is easy to use in practical approach but it has some inherent disadvantages as well. Specifically, it is useful for rectangular design patches and it ignores field variations along the radiating edges [5]. The cavity model is more accurate but at the same time more complex. However, it gives good physical insight and is rather difficult to model coupling.

II.2.1. Field Distribution in a cavity Model

The cavity model of the Microstrip assumes that the patch and the ground plane are electric walls, and the periphery of the patch is a magnetic wall [3]. When the microstrip patch is provided power, a charge distribution is seen on the upper and lower surfaces of the patch and at the bottom of the ground plane (Figure II.2). This charge distribution is controlled by

two mechanisms-an attractive mechanism and a repulsive mechanism as discussed by Richards shown in chapter I (Figure I.4: Distribution of charge and current density).

- The attractive mechanism is between the opposite charges on the bottom side of the patch and the ground plane, which helps in keeping the charge concentration intact at the bottom of the patch.
- The repulsive mechanism is between the like charges on the bottom surface of the patch, which causes pushing of some charges from the bottom, to the top of the patch. As a result of this charge movement, currents flow at the top and bottom surface of the patch.

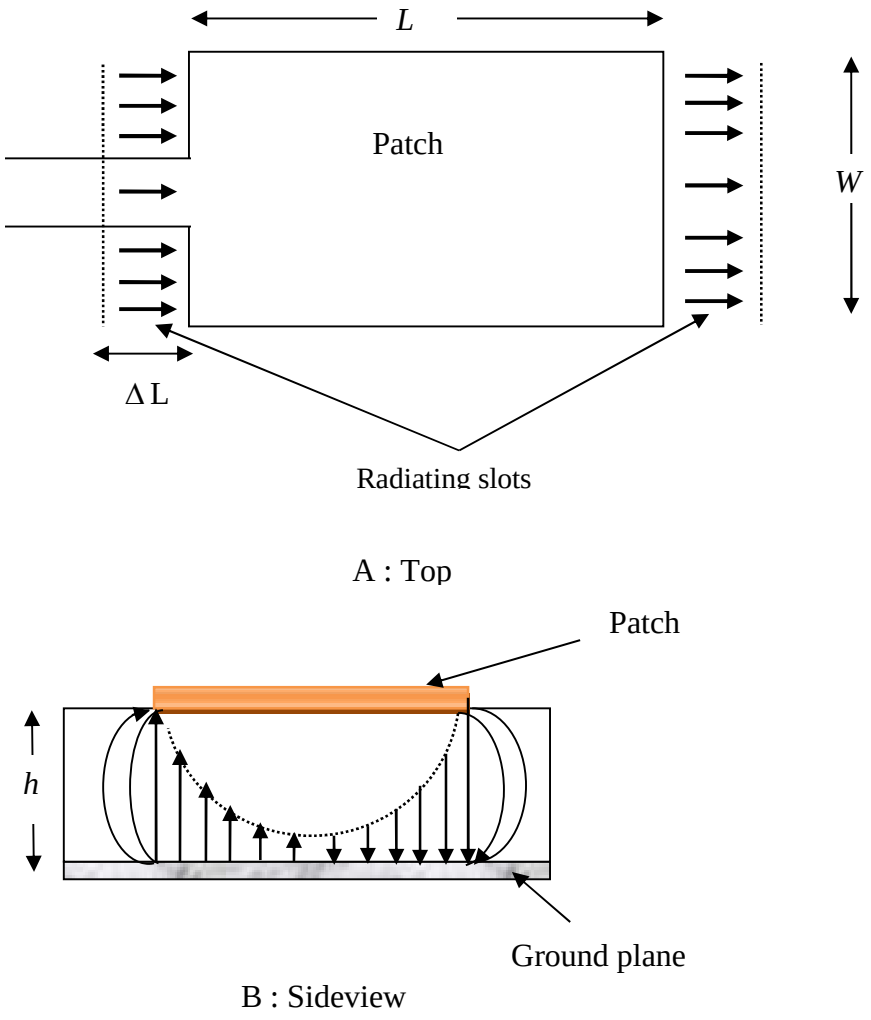

Figure II.2. The normal components of the electric field.

The cavity model assumes that the height to width ratio (i.e. height of substrate and width of the patch) is very small and as a result of this the attractive mechanism dominates and causes

most of the charge concentration and the current to be below the patch surface. Much less current would flow on the top surface of the patch and as the height to width ratio further decreases, the current on the top surface of the patch would be almost equal to zero, which would not allow the creation of any tangential magnetic field components to the patch edges. Hence, the four sidewalls could be modeled as perfectly magnetic conducting surfaces. This implies that the magnetic fields and the electric field distribution beneath the patch would not be disturbed. However, in practice, a finite width to height ratio would be there and this would not make the tangential magnetic fields to be completely zero, but they being very small, the side walls could be approximated to be perfectly magnetic conducting [6].

II.3. Mathematical formulation

This model basically treats the antenna as a cavity of thickness h and a conducting patch having dimensions L and W with electric walls on the top and bottom and magnetic walls around the perimeter of the patch. The radiation is assumed to occur from the slots formed by the periphery of the patch and ground plane [7].

The theoretical model is based on the following assumptions:

- The electric field is Z directed only, and the magnetic field has only the transverse components H_x and H_y in the region bounded by the patch metallization and the ground plane [8];
- The tangential component of the magnetic field is negligible at the edge of the patch [3];
- Because h (height of the substrate) is very thin ($h<<\lambda$), field in the interior region do not vary with Z coordinates for all frequencies [9];
- The electric current in the microstrip patch has no component normal to the edge of the patch at any point [9].
- Electrical walls in the $z=0$ and $z=h$ planes are ideal [10];
- Magnetic walls in the $y=0$, $y=W$, $x=0$, $x=L$ planes are ideal [11];
- Let $\vec{A}$ be the current density of the feed, assumed to be directed along Z;
- Since $h<<\lambda$, we assume A to be independent of Z [11].

In a homogeneous source free medium, $\vec{A}_z$ satisfies the wave equation:

$$\vec{\nabla}\cdot\vec{A}=\frac{\partial A_x}{\partial x}+\frac{\partial A_y}{\partial y}+\frac{\partial A_z}{\partial z}=-j\mu \tag{II.1}$$

In the cavity (region between patch and conducting plane)

$$\vec{\nabla}\cdot\left(\vec{\nabla}\times\vec{\mathrm{A}}\right)=\vec{\nabla}\left(\vec{\nabla}\cdot\vec{\mathrm{A}}\right)-\vec{\nabla}^2\,\vec{\mathrm{A}}^2 \tag{II.2}$$

$$\vec{\nabla}\cdot\vec{\mathrm{A}}=0 \tag{II.3}$$

$$\vec{\nabla}\times\left(\vec{\nabla}\times\vec{\mathrm{A}}\right)=\mu^{\,2}\text{«£}\,\vec{\mathrm{A}} \tag{II.4}$$

$\vec{A}_z$ Is obtained by first solving the homogeneous equation subject to the boundary conditions, the solution to the inhomogeneous equation is then obtained by superposition. Homogeneous equation:

$$\left(\nabla^2+\vec{}\;^2\right)\vec{\mathrm{A}}_z=0 \tag{II.5}$$

Where $=\mu\sqrt{\text{«£}}$

$$\frac{\partial^2\mathrm{A}_z}{\partial x^2}+\frac{\partial^2\mathrm{A}_z}{\partial y^2}+\frac{\partial^2\mathrm{A}_z}{\partial z^2}+\;^2\mathrm{A}_z=0 \tag{II.6}$$

Whose solution written general using the separation of variable:

$$\mathrm{A}_z=f(x)\cdot g(x)\cdot h(x) \tag{II.7}$$

With:

$$B^2=\;_x^{\,2}+\;_y^{\,2}+\;_z^{\,2} \tag{II.8}$$

The solutions of (II.1; II.2) are harmonic functions:

$$f(x)=\mathrm{A}_1\cos(\;_x x)+C_1\sin(\;_x x) \tag{II.9}$$

$$g(x) = A_2 \cos(\ _y y) + C_2 \sin(\ _y y) \quad \text{(II.10)}$$

$$h(x) = A_3 \cos(\ _z z) + C_3 \sin(\ _z z) \quad \text{(II.11)}$$

$$A_z = \left[A_1 \cos(\beta_x x) + C_1 \sin(\ _x x) \cdot A_2 \cos(\ _y y) + C_2 \sin(\ _y y) \cdot A_3 \cos(\ _z z) + C_3 \sin(\ _z z)\right] \quad \text{(II.12)}$$

Where β_x and β_y and β_z are wave numbers along the *x*, *y*, *z* directions, respectively these will be determined subject conditions the electric and magnetic field within the cavity are related to the vector potential A_z.

$$E_x = -j\frac{1}{\mu\varepsilon}\frac{\partial^2 A_z}{\partial x \partial z} \quad \text{(II.13)}$$

$$E_y = -\frac{1}{\mu\varepsilon}\frac{\partial A_z}{\partial x \partial z} \quad \text{(II.14)}$$

$$E_z = -j\frac{1}{\mu\varepsilon}\left(\frac{\partial^2}{\partial x} + \ ^2\right)A_z \quad \text{(II.15)}$$

$$H_x = \frac{1}{\ }\frac{\partial A_z}{\partial y} \quad \text{(II.16)}$$

$$H_y = \frac{1}{\ }\frac{\partial A_z}{\partial x} \quad \text{(II.17)}$$

$$H_z = 0 \quad \text{(II.18)}$$

The primed coordinates x', y', z' are used to represent the field within the cavity.

$$E_x = (z' = 0, h) = 0 \quad \text{(II.19)}$$

$$H_x = (y' = 0, W) = 0 \quad \text{(II.20)}$$

$$H_y = (x' = 0, L) = 0 \quad \text{(II.21)}$$

Where A_{mnp} represents the amplitude coefficients of each m, n, p mode, the wave numbers $\beta x, \beta y, \beta z$ are equal to:

$$C_3 = 0 \tag{II.22}$$

$$\begin{cases} {}_z = \dfrac{p®}{h} & \text{(II.23)} \\ C_2 = 0 & \text{(II.24)} \\ {}_y = \dfrac{n®}{W} & \text{(II.25)} \\ C_1 = 0 & \text{(II.26)} \\ {}_x = \dfrac{m®}{L} & \text{(II.27)} \end{cases}$$

The final from for the vector potential within the cavity is:

$$\mathrm{A}_z = \mathrm{A}_{mnp} \cos\left({}_x x' \right) \cdot \cos\left({}_y y' \right) \cdot \cos\left({}_z z' \right) \tag{II.28}$$

where m, n, p represent respectively the number of half cycle variations along the x, y, z direction since the wave numbers βx and βy and βz are subject to constraint equation.

$${}_x^2 + {}_y^2 + {}_z^2 = \left(\frac{m®}{L}\right)^2 + \left(\frac{n®}{W}\right)^2 + \left(\frac{p®}{h}\right)^2 = \mu^2 «£ = B^2 \tag{II.29}$$

$$B = \mu\sqrt{«£} = 2®f\sqrt{«£} \tag{II.30}$$

$$f = \frac{B}{2®\sqrt{«£}} \tag{II.31}$$

The resonant frequencies for the cavity are by:

$$f_{mnp} = \frac{1}{2®\sqrt{«£}} \sqrt{\left(\frac{m®}{L}\right)^2 + \left(\frac{n®}{W}\right)^2 + \left(\frac{p®}{h}\right)^2} \tag{II.32}$$

II.4. Modified cavity model of rectangular MSA

An MSA in its simplest form consists of a radiating patch on one side of a dielectric substrate and a ground plane on the other side. The top and side views of a rectangular MSA (RMSA) are shown in Figure II.3, thickness with dimensions (L, W) along two axes (x, y) respectively is printed on a grounded dielectric stab of thickness the substrate is characterized by the free space permeability «$_0$ and permittivity £$_0$, £$_r$ [10].

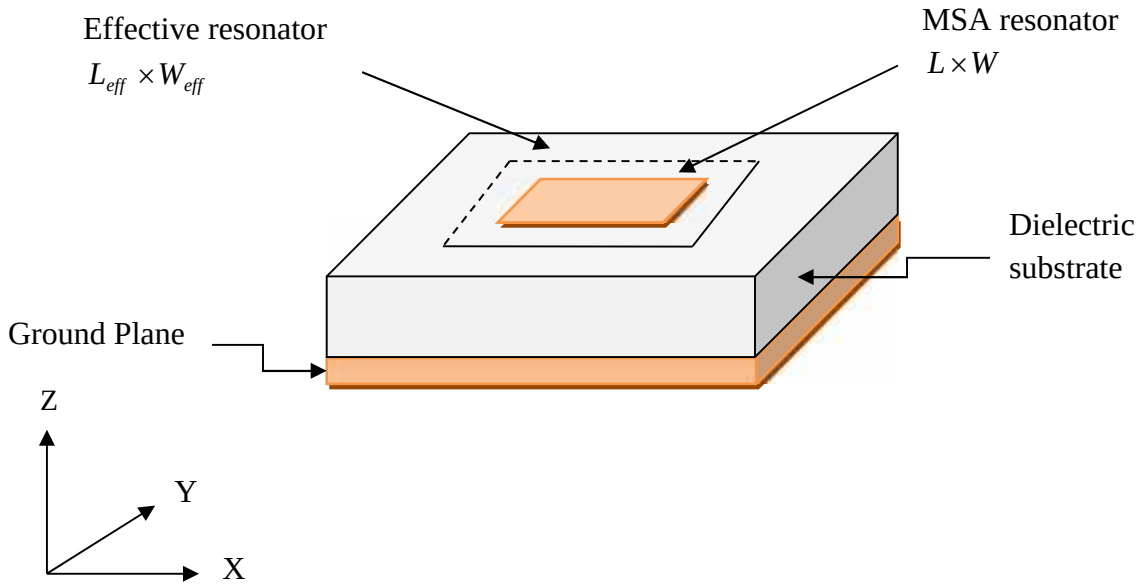

Figure II.3. Rectangular microstrip patch geometry used for cavity model analysis.

The resonant frequency of the rectangular microstrip patch antenna for mode is given by:

$$f_{mn} = \frac{1}{2® \cdot \sqrt{«£}} \cdot \sqrt{\left(\frac{m®}{L}\right)^2 + \left(\frac{n®}{W}\right)^2} \qquad \text{(II.33)}$$

The fringing fields along the width can be modeled as radiating slots and electrically the patch of the microstrip antenna looks greater than its physical dimensions. The dimensions of the patch along its length have now been extended on each end by a distance ΔL, which is given empirically by Hammerstad as [1]:

$$L_{eff} = L + 2\Delta L \qquad \text{(II.34)}$$

$$W_{eff} = W + 2\Delta W \tag{II.35}$$

$$\Rightarrow \Delta L = 0{,}412h\frac{£_r + 0{,}3}{£_r - 0{,}258}\left(\frac{W/h + 0{,}264}{W/h + 0{,}813}\right) \tag{II.36}$$

A similar expression with appropriate modifications can be used for effective width, consequently, the resonant frequency of rectangular microstrip antenna can be calculated with (II.33) by replacing equation (II.34), (II.36) to (II.33).

II.4.1. Analysis of the tapered MSA using the cavity model

The tapered MSA considered is shown in Figure II.4.The rectangular patch has width W and length L and s printed on an anisotropic substrate (region 1). The thickness of the conducting patch is neglected. The substrate height varies linearly from h1 to h_2, where the non radiating edge is on a plane that intersects the ground plane with an angle, · (Figure II.5). Region 2 is air–filled with parameters $£_0$ and $«_0$ denoting the free space values of permittivity and permeability, respectively.

The electric permittivity tensor of the dielectric substrate is diagonal, with the optical axis along they direction, and is given by [10].

$$£\tilde{} = \begin{bmatrix} £_2 & 0 & 0 \\ 0 & £_1 & 0 \\ 0 & 0 & £_2 \end{bmatrix} \tag{II.37}$$

Where the electric permittivity component along the optical axis is $£_1 = £_{r1}£_0$, and those on the plane perpendicular to it are equal to $£_2 = £_{r2}£_0$

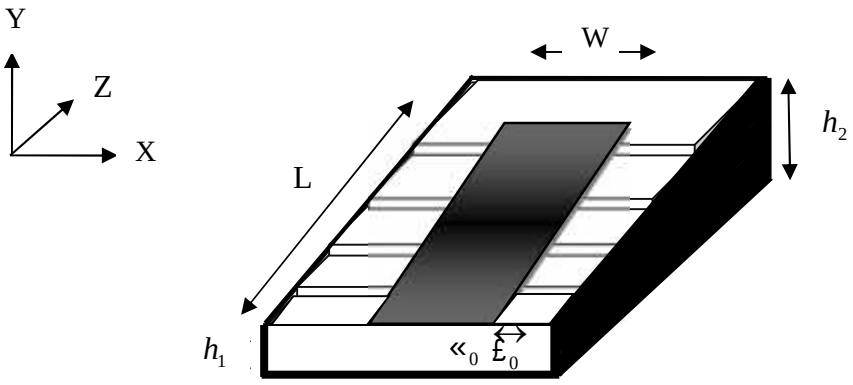

Figure II.4. Tapered microstrip patch antenna.

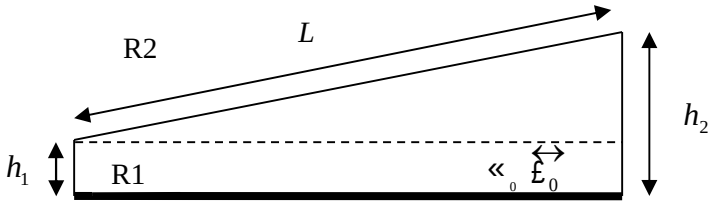

Figure II.5. Side view of the considered structure.

The effective dielectric constant is obtained by cavity model method, and is given by:

$$\varepsilon_{eff} = \frac{1}{2}\cdot\left[\left(\frac{z=0}{k_0}\right)^2 + \left(\frac{z=L}{k_0}\right)^2\right] \tag{II.45}$$

Here, ΔL is calculated as follows:

$$\Delta L = \frac{\Delta L_{1(z=0)} + \Delta L_{2(z=L)}}{2} \tag{II.46}$$

Where:

$$\Delta L_i = 0{,}412 h_i = \frac{(\varepsilon_{eff_i} + 0{,}3)}{(\varepsilon_{eff_i} - 0{,}258)}\frac{(w/h_i + 0{,}264)}{(w/h_i + 0{,}813)}, \quad i = 1{,}2 \tag{II.47}$$

With: $h_2 = h_1 + L\,\mathbf{sin}\cdot$

Where · is the angle between the ground plane and the plane containing the patch (FigureII.5). In this approach, we calculate $£_{eff}$ and ΔL for the narrow end ($z = 0$) and for the wide end $z = L$), respectively, to yield a more accurate design of the tapered microstrip antenna.

II.4.2. Resonant Frequency of HTS microstrip antenna

The resonant frequency of HTSMAs will vary with temperature due changes in the surface reactance of the HTS thin films used to fabricate the microstrip patches. This change in resonant frequency can be determined using a modified cavity model of the microstrip patch antenna, by considering the effective dielectric constant [12].

$$£_{eff} = £_{req}\left[1 + \frac{a_f}{h_{eq}} coth\left(\frac{t}{a_f}\right)\right] \tag{II.48}$$

For an HTS film with thickness t and the permittivity equivalent $£_{eff}$. For a homogeneous superconductor, the temperature dependence of the magnetic penetration depth a_f , can be modeled by the Gorter-Casimir two-fluid model as [12]

$$a_f = a_0\left[1 - \left(\frac{T}{T_c}\right)^4\right]^{-\frac{1}{2}} \tag{II.49}$$

where T is the operating temperature and T_c is the transition temperature of the superconductor film. Although this expression is not empirically correct for HTS films because of their inhomogeneity, it is still useful for modelling the temperature behavior of a_f for HTS, especially at temperatures far below T_c [13].

II.5. Conclusion

The present work deals with the analysis and design of tapered microstrip patch antenna printed on anisotropic dielectric substrate. The cavity model combined with London's equations and the Gorter-Casimir two-fluid model has been improved to investigate the resonant characteristics of high Tc superconducting tapered microstrip patch in the case where the patch is printed on uniaxial anisotropic substrate materials. In this chapter, we exploit the cavity model to design and analyze a rectangular microstrip antenna; the antenna

is accommodated for a resonant cavity having two perfect electric walls, corresponding to perfectly conductive surfaces, and four magnetic sidewalls. The inclusion of the edge fields in the mathematical formulation makes it possible to obtain a reliable model for thin substrates as well as for thick substrates. This allows us to study in this chapter the analytical study for a tapered microstrip patch antenna. We will discuss the results with Matlab in the next chapter.

III.6. References

[1] C. A. Balanis, Antenna Theory: Analysis and Design, 3rd ed. New York: Wiley, 2005.

[2] K. K. Parashar, V. K. Singh, and R. Tiwari, "Microstrip patch antenna for WiMAX/WLAN applications," *Advance Physics Letter*, vol. 1, no. 1, pp. 34-37, 2014.

[3] A. T. Gobien, " investigation of low profile antenna designs for use in hand-held radios" These de doctorat, virginia tech, - 1997.

[4] R.C. Johnson, and Jasik, H.: '*Antenna engineering handbook*', New York, McGraw-Hill Book Company, USA, 1984.

[5] Y. Huang, and Boyle, K.: '*Antennas: from theory to practice*', John Wiley & Sons, USA, 2008.

[6] J.R. James, Hall, P.S., and Wood, C., "*Microstrip antenna: theory and design*", let, Stevenage, Herts., Peter Peregrinus, Ltd, England, 1986.

[7] D.M. Pozar, "Microwave engineering", Wiley, USA, 2012.

[8] E.O. Hammerstad, "Equations for microstrip circuit design", *IEEE 5th European Microwave Conference*, pp. 268-272, Hamburg, Germany, 1975.

[9] B. Katia and B. Taoues, "Etude des antennes planaires avec le modèle de la cavité et le modèle de la ligne de transmission," Mémoire de Master, Université de TiziOuzou, Algerie, 2013.

[10] A. Mhamdi, S. Bedra, R. Bedra, and S. Benkouda, "CAD cavity model analysis of high Tc superconducting rectangular patch printed on anisotropic substrates," 5th International Conference on Electrical Engineering-Boumerdes (ICEE-B). 2017

[11] D. M. Pozar, 1987,''Radiation and scattering from a microstrip patch on a uniaxial substrate,''1987.

[12] M. A. Richard, K. B. Bhasin, and P. C. Claspy, "Superconducting microstrip antennas: an experimental comparison of two feeding methods," *Antennas and Propagation, IEEE Transactions on*, vol. 41, pp. 967-974, 1993.

[13] S. Bedra, R. Bedra, S. Benkouda, and T. Fortaki, "Efficient CAD model to analysis of high Tc superconducting circular microstrip antenna on anisotropic substrates," *Advanced Electromagnetics*, vol. 6, pp. 40-45, 2017.

Chapter III

Superconducting Materials

III.1. Introduction

Nowadays, the need for higher data transmission rate (Gb/s) of wireless communication systems motivates the usage of millimeter wave frequency bands (e.g., 57– 64 GHz in USA, 59–66 GHz in Japan). Microstrip antennas of various shapes have recently received much attention and have been widely used in the range of millimeter-wave frequencies. The discovery of new superconducting materials facilitates the development of microwave and millimeter-wave devices with better performance than conventional devices, where have a great effect on the performance of microstrip antennas, due to the much lower surface resistance compared with normal conductor and high transition temperature over the boiling point of liquid nitrogen. High Tc (High critical temperature) superconducting microstrip patch antennas have higher gain than their normal counterparts, but they suffer from the extremely narrow bandwidth, which severely limits their application [1].

Superconductivity is a very curious phenomenon characterized by a phase transition at a critical temperature (*T*c) in which the conducting phase is in equilibrium with the superconducting phase. The most important properties of the superconducting phase are: zero resistance, ideal diamagnetism (Meissner effect), magnetic flux quantization and persistent current in superconducting rings, cylinders or coils. On the other hand, many effects are found in superconducting constrictions as well as in junctions between two superconductors or in junctions between a superconductor and a conductor. These effects are known as “Josephson effects”: It is possible to occur tunneling of Cooper pairs across a thin insulator between two superconductors and thus a superconducting current may be maintained across the junction [2].

Due to all the effects mentioned above, superconducting devices may be projected for an enormous number of practical applications. Superconducting wires can be used for power transmission and in other applications when zero resistance is required. Persistent currents can be used in superconducting magnets and in SMES (superconducting magnetic energy storage). Devices based on the Josephson effects are actually been used in very sensitive. Superconducting magnets has been used in particle accelerators. However, the actual use of these superconducting devices is limited by the fact that they must be cooled to low temperatures to become superconducting [2].

The advantages of using the superconducting materials at high frequencies are: very small losses which mean low attenuation and low noise, smaller devices due to the lower losses, which leads to larger integration density, and the propagation time can be greatly reduced because of the smaller size and the shorter interconnects [3].

III.2. History of the Discovery

Superconductors, materials that have no resistance to the flow of electricity, are one of the last great frontiers of scientific discovery. Not only have the limits of superconductivity not yet been reached, but the theories that explain superconductor behavior seem to be constantly under review, where:

In 1911, superconductivity was first observed in mercury by Dutch physicist Heike Kamerlingh Onnes of Leiden University. When he cooled it to the temperature of liquid helium, 4.2 degrees Kelvin (-452F, -269°C), its resistance suddenly disappeared at low temperature, (Figure III.1). The temperature below which this effect occurs is called the temperature of the transition (transformation) into the superconducting state (*T*c) or the critical or transition temperature. The Kelvin scale represents an "absolute" scale of temperature. Thus, it was necessary for Ones to come within 4 degrees of the coldest temperature that is theoretically attainable to witness the phenomenon of superconductivity [4]-[5].

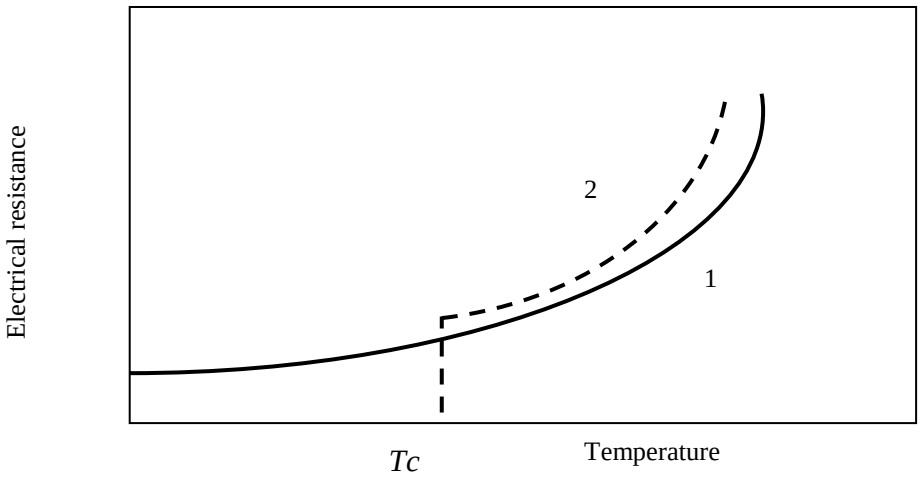

Figure III.1. Dependence of the electrical resistance on the measuring temperature (schematic): normal metal (1); superconductor (2).

In 1933, the next great milestone in understanding how matter behaves at extreme cold temperatures occurred. When German researchers Walther Meissner and Robert Ochsenfeld discovered that a superconducting material will repel a magnetic field. A magnet moving by a conductor induces currents in the conductor. This is the principle on which the electric generator operates. But, in a superconductor the induced currents exactly mirror the field that would have otherwise penetrated the superconducting material - causing the magnet to be repulsed (any external magnetic field is completely unable to penetrate into the inside of the superconductor, and if the transition into the superconducting state takes place in a magnetic field, then the field is expelled from the superconductor). This phenomenon is known as strong diamagnetism and is today often referred to as the "Meissner effect". The Meissner effect is so strong that a magnet can actually be levitated over a superconductive material [5].

In 1957, the first widely-accepted theoretical understanding of superconductivity was advanced by American physicists John Bardeen, Leon Cooper, and John Schrieffer. Their Theories of Superconductivity became known as the BCS theory derived from the first letter of each man's last name - and won them a Nobel Prize in 1972. The mathematically complex BCS theory explained superconductivity at temperatures close to absolute zero for elements and simple alloys. However, at higher temperatures and with different superconductor systems, the BCS theory has subsequently become inadequate to fully explain how superconductivity is occurring [6].

In 1964 Bill Little of Stanford University had suggested the possibility of organic (carbon-based) superconductors. The first of these theoretical superconductors was successfully synthesized in 1980 by Danish researcher Klaus Bechgaard of the University of Copenhagen and three French team members [6].

In 1986, the discovery of Bednorz and Müller of an oxide superconductor with critical temperature (Tc) approximately equal to 35 K, has given a novel impetus to this fascinating subject. Since this discovery, there are a great number of laboratories all over the world involved in research of superconductors with high Tc values, the so-called “high-Tc superconductors”. The discovery of a room temperature superconductor has been a long standing dream of many scientists.

Until 2011, one hundred years after the first Kamerlingh Onnes' discovery, the highest Tc value is approximately equal to 135 K at 1 atm. The knowledge of the microscopic mechanisms of high-Tc superconductors should be a theoretical guide in the researches of room temperature superconductivity [7].

Twenty-seven metals are superconductors; superconductivity also exists in more than a thousand compounds and alloys, where temperatures of transition into the superconducting state range from 0.01 to 21° K.

III.3. Properties of superconducting materials

III.3.1. Zero resistance

After H. KamerlinghOnnes had managed to liquefy Helium, it became possible to reach temperatures low enoughto achieve superconductivity in some chemical elements. In 1911, he found that the static (dc) resistivity ofmercury abruptly fell to zero at a critical temperature Tc of about 4.2 K (Figure III.2).The temperature at which a superconductor loses resistance is called its superconducting transition temperature or critical temperature Tc, this temperature is different for each metal, where separates the behavior of the normal state of the material from that of its superconducting state.

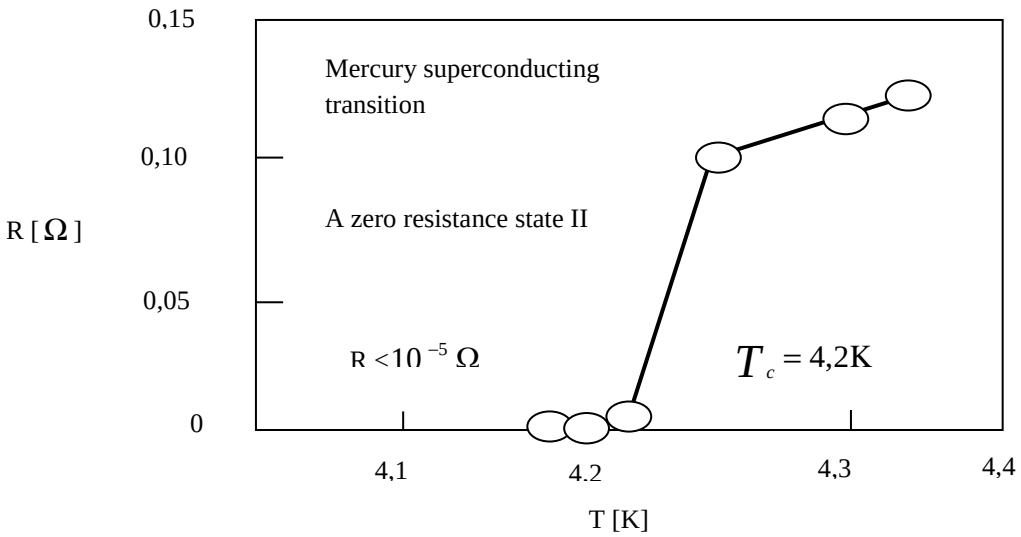

Figure III.2. The resistance of mercury measured by Onnes.

For a perfectly pure metal, where the electron motion is impeded only by the thermal vibrations of the lattice, the resistivity should approach zero as the temperature is reduced towards 0K. Any real specimen of metal cannot be perfectly pure and will contain some impurities. The transition is very sharp in pure materials (as narrow as 10^{-3} K), broader when impurities are present [8].

III.3.2. Meissner effect

Because the zero resistance features of superconductors was discovered first, it is widely believed that this is the most fundamental property of superconductors. Actually, the Meissner effect is of equal or greater significance, and plays a central role in the magnetic phenomena associated with superconductivity.

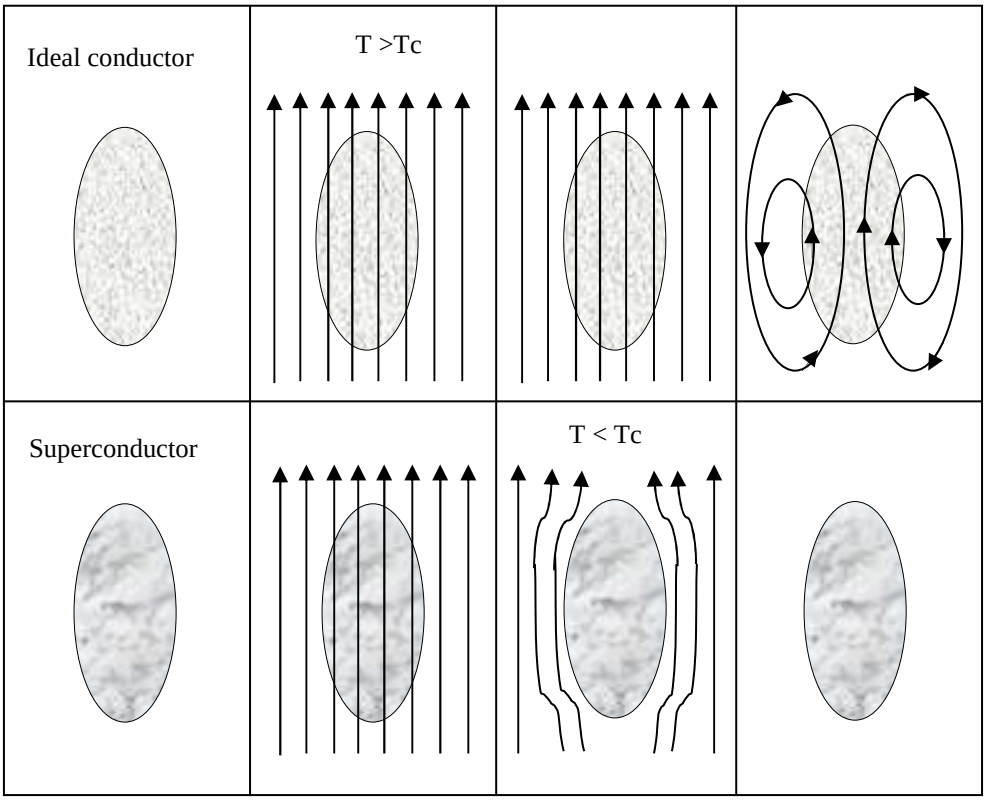

Figure III.3. The Meissner effect.

In 1933, Walter Meissner and Robert Ochsenfeld discovered a magnetic phenomenon that showed that superconductors are not just perfect conductors. Figure III.3 illustrates a thought experiment that highlights this difference. Where it's found that the superconductor expels the magnetic field from inside it, while the ideal conductor maintains its interior field. Note that energy is needed by the superconductor to expel the magnetic field. This energy comes

from the exothermic superconducting transition. Switching off the field induces currents in the ideal conductor that prevent changes in the magnetic field inside it – by Lenz's law. However, the superconductor returns to its initial state, i.e. no magnetic field inside or outside it [9].

Meissner will explain this property of the superconductor by the appearance of super currents on the surface of the material (Lenz's law) creating a magnetic flux which opposes exactly the external magnetic field:

$$\vec{B} = \mu_0 \vec{H}_a + \vec{B}_s = \mu_0 \left(\vec{H}_a + \vec{H}_a X \right) \qquad \text{(III.1)}$$

III.3.3. Magnetic Levitation

The magnetic levitation force (F) of a superconductor is dependent on its manufacturing process. The F of the MG-processed superconductors is very large. For example, the F of the single-grain bulk superconductors measured at 77 K is as large as 50–150 N, depending on the dimension of a permanent magnet. It indicates that the weight of several tons can be levitated using the superconductors and magnets. F of superconductors is given by equation:

$$F = m\left(\frac{dH}{dx}\right) \qquad m = \mathrm{M}_v,\ \mathrm{M} = \mathrm{A}J_c^r \qquad \text{(III.2)}$$

Where m is the magnetic moment of a superconductor, dH/dx is a field gradient produced by a magnet, M is the magnetization per unit volume, v is the volume, A is the constant related to the sample geometry, Jc is the critical current density of a superconductor and r is the radius of the shielding current loop (grain size of the superconductor). In addition to Jc and r, other experimental parameters such as the size of the superconductor, the magnetic strength of the magnet used for the measurement and the cooling method for superconductors affect F [10].

III.4. Types of superconductors

Prior to about 1960, superconductors were interesting from the point of view of physics, but had no practical applications because they couldn't carry any significant amount of current.

Only when a new class of superconductors was discovered did practical applications become possible. All homogeneous superconductors separated into two groups: superconductors of the first group, which include all pure metals except niobium and vanadium, superconductors of the second group, which include niobium, vanadium, and all other superconducting alloys and compounds.

The two groups are distinguished as type I and type II superconductors, also known as soft and hard superconductors, because of the dramatic difference in their magnetic and current-carrying properties. There are such enormous differences between J_C in the two types that an entire industry is based on type II superconductors, while type I superconductors have only very limited applications [11].

III.4.1. Type I superconductors

The type I "soft" superconductors acts as a perfect diamagnetic material and obeys Meissner effect and are well described by the BCS theory with lead bismuth alloys starting in 1930.BCS theory suggests that electrons team up in "Cooper pairs" in order to help each other overcome molecular obstacles. For a type I superconductor, critical current is simply a consequence of the critical magnetic field.

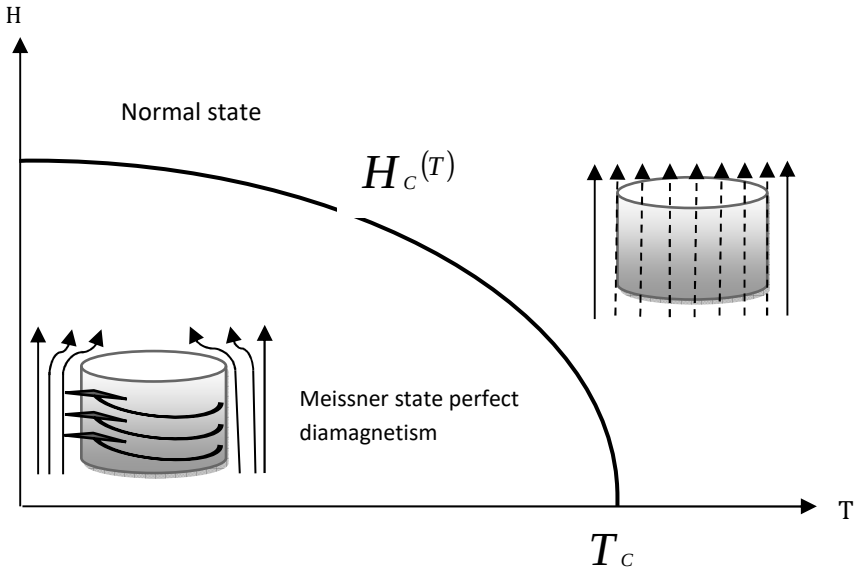

Figure III.4. Variation of the critical field as a function of temperature for a type I superconductor.

Since is low in type I superconductors, their critical current densities are likewise low, then there is only one critical magnetic field Hc1, and so only two states: superconducting or normal (Figure III.4), where the magnetic field partially penetrates the material along, called the London length, where supercurrents develop. This is why type I superconductors have not been of interest to the electric utilities or magnet builders [5] [11]. The critical magnetic field at any temperature below the critical temperature is given by the relationship:

$$H_c(T) = H_c^0\left(1-\left(\frac{T}{T_c}\right)^2\right) \qquad \text{(III.3)}$$

With: H_C^0 The field at zero temperature

III.4.2. Type II superconductors

Superconductors of the second group were first discovered in 1930, as in the case of those of the first group, they are characterized by the temperature of the transition into the superconducting state (Tc).

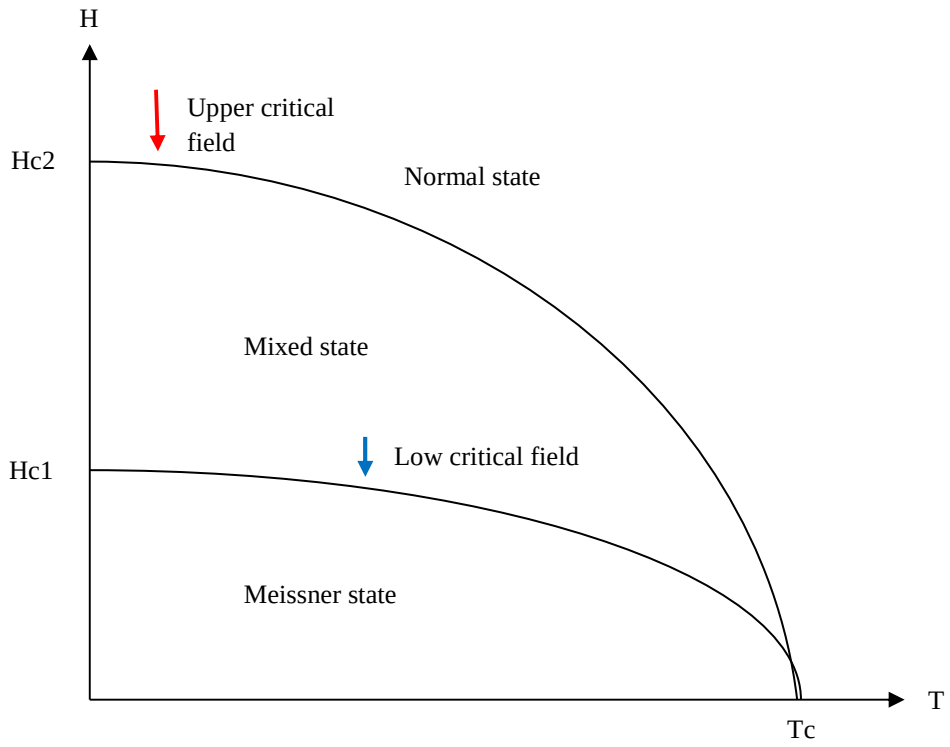

Figure III.5. Variation of the critical field as a function of temperature for a type II superconductor.

The special feature of superconductors of this group as compared with the former is the existence of two critical fields (Figure III.5): lower *H*c1 and upper *H*c2. Before reaching *H*c1, these superconductors behave in the same way as those of the first group [12].

The presence of two critical fields makes things more complicated. They are three zones to consider:

- Zone 1 ($H < H_{c1}$): The behavior is analogous to that of type I superconductors.
- Zone 2 ($H_{c1} < H < H_{c2}$): The state mixed is characterized by partial penetration of the field magnetic in the form of a vortex, and therefore a partial diamagnetism.
- Zone 3 ($H > H_{c2}$): The material returns to state normal.

III.5. Theory of Superconductivity

III.5.1. London theory

In 1935, F. and H. London proposed a phenomenological theory for the electrodynamics properties of superconductors. It is based on a two-fluid picture: For unspecified reasons, the electrons from a normal fluid of concentration *nn* and a super-fluid of concentration ns, where $n_n + n_s = n$ = N/V. Such a picture seemed quite plausible based on Einstein's theory of Bose-Einstein condensation (1925), although nobody understood how the fermionic electrons could form a superfluid. The normal fluid is postulated to behave normally, i.e., to carry an Ohmic current [13].

$$j_n = \sigma_n E \tag{III.4}$$

Governed by the Drude conductivity

$$\sigma_n = \frac{e^2 n_n \tau}{m} \tag{III.5}$$

The London's have assumed that *nn* and n_s are both uniform (constant in space) and stationary (constant in time). These are serious restrictions of London theory, which will be overcome by Ginzburg-Landau theory. With the supercurrent

$$j_s = -e n_s v_s \tag{III.6}$$

and Newton's equation of motion

$$\frac{d}{dt}v_s = \frac{F}{m} = -\frac{eE}{m}, \tag{III.7}$$

we then obtain

$$\frac{\partial j_s}{\partial t} = \frac{e^2 n_s}{m} E \tag{III.8}$$

The same follows from the Boltzmann equation in the absence of scattering. This is the First London Equation:

$$\frac{\partial}{\partial t}\nabla \times j_s = \frac{e^2 n_s}{m}\nabla \times E = -\frac{e^2 n_s}{mc}\frac{\partial B}{\partial t} \tag{III.9}$$

This equation can be integrated in time to give:

$$\nabla \times j_s = -\frac{e^2 n_s}{mc} B + C(r) \tag{III.10}$$

Where the last term represents a constant of integration at each point r inside the superconductor and C(r) should be determined from the initial conditions. If we start from a superconducting body in zero applied magnetic field, we have $J_s \equiv 0$ and $B \equiv 0$ initially so that C(r) = 0.

To account for the flux expulsion, the London's postulated that $C \equiv 0$ regardless of the history of the system. This leads to

$$\nabla \times j_s = -\frac{e^2 n_s}{mc} B, \tag{III.11}$$

This is the Second London Equation, Taking the curl of Ampere's law

$$\nabla \times B = \frac{4\pi}{c} j_s + \frac{4\pi}{c} j_n \tag{III.12}$$

(There is no displacement current in the stationary state) we get.

$$\nabla\times\nabla\times B=-\frac{4\pi e^2 n_s}{mc^2}B+\frac{4\pi}{c}\sigma_n\nabla\times E=-\frac{4\pi e^2 n_s}{mc^2}B-\frac{4\pi}{c}\sigma_n\frac{\partial B}{\partial t} \quad \text{(III.13)}$$

We drop the last term since we are interested in the stationary state and use an identity from vector calculus (BAC-CAB rule), which gives

$$-\nabla(\nabla.B)+\nabla^2 B=\frac{4\pi e^2 n_s}{mc^2}B. \quad \text{(III.14)}$$

With the London penetration depth

$$\lambda L=\sqrt{\frac{mc^2}{4\pi e^2 n_s}} \quad \text{(III.15)}$$

III.5.2. Ginzburg–Landau theory

It is convenient in developing an understanding of superconductivity to introduce the 'condensate wave function' or Ginsburg–Landau wave function. This can be formally defined in terms of the correlation function to which we have already referred, but in essence it is a complex function, ψ, the phase of which is the phase of the wave function of the condensed pairs and the amplitude of which is proportional to the local concentration of condensed pairs. The function ψ obeys the Ginsburg–Landau equations when the temperature is near Tc, at lower temperatures these equations cease to be strictly correct, but they still provide a correct qualitative description. One of the GL equations gives the supercurrent density [14].

$$J(r)=\frac{ie\hbar}{2m}\left(\psi^*\nabla\psi-\psi\nabla\psi^*\right)-\frac{2e^2}{m}\psi\psi^*A(r) \quad \text{(III.16)}$$

Since the modulus of ψ is a measure of the density of condensed electrons it also a measure of the extent of the superconducting ordering. Indeed Ginsburg and Landau originally introduced ψ as a (complex) 'order parameter,' and it is frequently referred to in this way. Often it is referred to in other ways: 'the gap parameter,' since it is proportional to the energy gap in a spatially homogeneous situation, or the 'pair potential,' since it appears as a self-consistent potential in some formulations of the theory of superconductivity.

III.5.3. BCS theory

BCS stands for Bardeen, Cooper and Schrieffer. The BCS theory explains the super conductivity of only TYPE I superconductors and DOES NOT explain TYPE II superconductors. The aim of BCS theory is to provide a satisfactory explanation to the superconductivity of TYPE I superconductors.

III.5.3.1. Cooper Pairs

The basic idea that even a weak attraction can bind pairs of electrons into a bound state was presented by cooper in 1956.

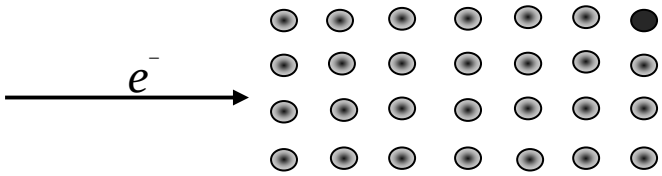

First electron approach a section of the crystal lattice.

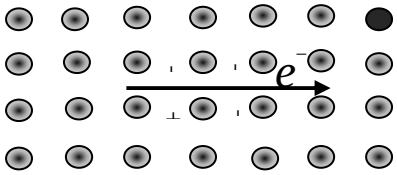

First electron deforms part of the lattice electrostatically.

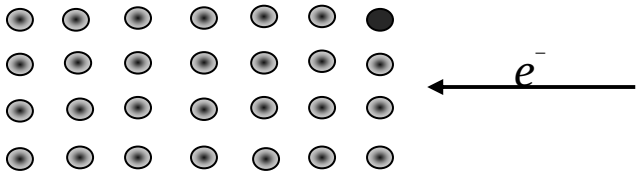

Second electron is attracted to the net positive charge of the deformation.

Figure III.6. Classical description of the coupling of a Cooper pair.

The central feature of the BCS theory is that two electrons in the superconductor are able to form a bound pair called a Cooper pair if they somehow experience an attractive interaction between them. This notion at first sight seems counterintuitive since electrons normally repel one another because of their like charges. This may sound very strange, but it has been verified experimentally. Cooper pairs are formed due to interaction between electrons and a

phonon. A phonon is quanta of vibration energy. Normally, electrons will have too much energy to stay in a Cooper pair (Figure III.6), however as the temperature is lowered sufficiently, electrons may be able to form Cooper pairs, as thermal vibrations will freeze and resistance will go to zero [15].

III.6. Superconductors Applications

III.6.1. Superconducting Magnets

Type II superconductors such as niobium-tin and niobium-titanium are used to make the coil windings for superconducting magnets. These two materials can be fabricated into wires and can withstand high magnetic fields. Typical construction of the coils is to embed a large number of fine filaments (20 micrometers diameter) in a copper matrix. The solid copper gives mechanical stability and provides a path for the large currents in case the superconducting state is lost. These superconducting magnets must be cooled with liquid helium.

Superconducting magnets can use solenoid geometries as do ordinary electromagnets. Most high energy accelerators now use superconducting magnets. The proton accelerator at Fermi lab uses 774 superconducting magnets in a ring of circumference 6.2 kilometers. They have also found wide application in the construction of magnetic resonance imaging (MRI) apparatus for medical imaging.

III.6.2. Superconducting Transmission Lines

Since 10% to 15% of generated electricity is dissipated in resistive losses in transmission lines, the prospect of zero loss superconducting transmission lines is appealing. In prototype superconducting transmission lines at Brookhaven National Laboratory, 1000 MW of power can be transported within an enclosure of diameter 40 cm. This amounts to transporting the entire output of a large power plant on one enclosed transmission line. This could be a fairly low voltage DC transmission compared to large transformer banks and multiple high voltage AC transmission lines on towers in the conventional systems. The superconductor used in these prototype applications is usually niobium titanium, and liquid helium cooling is required. Current experiments with power applications of high temperature superconductors focus on uses of BSCCO in tape forms and YBCO in thin film forms. Current densities

above 10,000 amperes per square centimeter are considered necessary for practical power applications, and this threshold has been exceeded in several configurations.

III.6.3. Superconducting Maglev Trains

While it is not practical to lay down superconducting rails, it is possible to construct a superconducting system onboard a train to repel conventional rails below it. The train would have to be moving to create the repulsion, but once moving would be supported with very little friction. There would be resistive loss of energy in the currents in the rails. Ohanian reports an engineering assessment that such superconducting trains would be much safer than conventional rail systems at 200 km/h. A Japanese magnetically levitated train set a speed record of 321 mi/h in 1979 using superconducting magnets on board the train. The magnets induce currents in the rails below them, causing a repulsion which suspends the train above the track.

III.6.4. Fault-Current Limiters

High fault-currents caused by lightning strikes are a troublesome and expensive nuisance in electric power grids. One of the near-term applications for high temperature superconductors may be the construction of fault-current limiters which operate at 77K. The need is to reduce the fault current to a fraction of its peak value in less than a cycle (1/60 sec). A recently tested fault-current limiter can operate at 2.4 kV and carry a current of 2200 amperes. It was constructed from BSCCO material.

III.6.5. Superconductors in NMR Imaging

Superconducting magnets find application in magnetic resonance imaging (MRI) of the human body. Besides requiring strong magnetic fields on the order of a Tesla, magnetic resonance imaging requires extremely uniform fields across the subject and extreme stability over time. Maintaining the magnet coils in the superconducting state helps to achieve parts-per-million special uniformity over a space large enough to hold a person, and ppm/hour stability with time.

III.6.6. Superconducting Motors

Superconducting motors and generators could be made with a weight of about one tenth that of conventional devices for the same output. This is the appeal of making such devices for

specialized applications. Motors and generators are already very efficient, so there is not the power savings associated with superconducting magnets. It may be possible to build very large capacity generators for power plants where structural strength considerations place limits on conventional generators. In 1995 the Naval Research Laboratory demonstrated a 167 hp motor with high-Temperature superconducting coils made from Bi-2223. It was tested at 4.2K and at liquid neon temperature, 28K with 112 hp produced at the higher temperature [5].

III7. Conclusion

In this chapter, a comprehensive study of superconducting materials has been studied since their discovery, as well as some of their properties and Classification according to certain bases; in addition we presented the theories, as well as important applications in daily life. What Superconductivity does is directing electricity without losing energy by unusual physical phenomenon, the formation of so-called Cooper pairs. In this state the electrons flow through the material without encountering obstacles. In many applications, engineers have taken advantage of this effect. Unfortunately, superconductivity occurs only at extremely low temperatures. To use the materials, therefore, extensive cooling systems are necessary. All the more astonished were scientists when they came across high-temperature superconductors a few years ago: with these substances, the effect already occurs at higher temperatures. Even if cooling is still necessary, it may be lower than with conventional conductors.

III.8. References

[1] Sami Bedra, S. Benkouda, R. Bedra, and T. Fortaki, "Inverted HTS rectangular patch antennas: Theoretical investigation," *Physica C: Superconductivity and its Applications*, vol. 580, p. 1353802, 2021.

[2] Adir Moysés Luiz, ‘’ A Model to Study Microscopic Mechanisms in High-Tc Superconductors,’’ doctorate thesis, *Instituto de Física, Universidade Federal do Rio de Janeiro Brazil*.

[3] Randa Bedra, "Etude d’une antenne supraconductrice couverte par une couche diélectrique," *Doctorate thesis, Université de Batna 2*, Algérie, 2018.

[4] Savitskii. E. M., V. V. Baron, Yu. V. Efimov, M. I. Bychkova, L. F. Myzenkova, Superconducting Materials, International Cryogenics Monograph Series,-Springer US (1973).

[5] Sawsan Ahmed Elhouri Ahmed & Mubarak Dirar Abdallah,'' A study on superconducting materials,'' , Global Journal of Engineering Science and Researches, University of Bahri-College of Applied & Industrial Sciences-Department of Physics-Khartoum –Sudan.

[6] James F., Annett (2004), ''Superconductivity, Superfluids and Condensates,'' Oxford, p. 58, ISBN 0-19- 850756-9.

[7] Mohamed Lamine Tounsi and M. C. E. Yagoub, "Efficient characterization of EMC shielding in anisotropic high-Tc superconducting devices for industrial applications," *International Journal of RF and Microwave Computer-Aided Engineering*, vol. 22, no. 1, pp. 116-123, 2012.

[8] Jatinder Vir Yakhmi, "Superconducting Materials and Their Applications: An interdisciplinary approach", IOP Publishing, Bristol, UK, 2021.

[9] Laurent-Patrick Levy , "Magnetisme et supraconductivite", Savaoirs InterEditions / CNRS Editions, France, 1997.

[10] Chan-Joong Kim, "Superconductor Levitation_ Concepts and Experiments", Springer Singapore, 2019.

[11] Thomas Sheehan , 'Introduction to High-Temperature Superconductivity', Springer , 1994.

[12] Abdellah Tnourji, ''Les caractéristiques des matériaux supraconducteurs, mémoire de Master, Université Clermont Auvergne , France , 2017.

[13] Bardeen J., L. N. Cooper, and J. R. Schrieffer," Theory of Superconductivity", Phys. Rev. 108, 1175, 1957.

[14] David A Cardwell, David S Ginley, ''Handbook of Superconducting Materials,'' Volume I: Superconductivity, Materials and Processes, 2000.

[15] Michael. Tinkham, ''Introduction to superconductivity,''2^{d} edition, international series in pure and applied physics.

IV.1. Introduction

Microstrip antennas have found pronounced acceptance in the electromagnetic and microwave theory practitioners due to their numerous advantages [1]. The interest in designing such microstrip antennas has increased because of light weight, smooth production, conformability, flexibility in shapes and integration with solid-state devices [2].Regarding the inherent narrow bandwidth of this type of antenna around their operating resonant frequencies, it is important to develop accurate algorithms for the computation of those resonant frequencies [3].To defeat this problem, several research has been performed so far and numerous techniques have been suggested to progress the antenna bandwidth such as increasing patch height, reducing substrate permittivity, using multiple resonators, etc. [4].During recent years, great interests have been shown in using microstrip antenna deposited on anisotropic substrate since the substrate anisotropy could have important applications on the operation of microstrip antennas [4].With the increasing complexity of geometry and material property, designing these antennas requires more and more dedicated and sophisticated computer aided-design (CAD)tools to predict the characteristics. The numerical methods such as Finite Element Method (FEM), Method of Moment (MoM), Finite Difference Time Domain (FDTD) method, etc. have been proven to be one of the most powerful CAD tools for solving this class of problems [5]. These techniques require high computational resources and also take lots of computation time. The computer-aided design (CAD) oriented cavity model is ideal for design purpose because it involves less mathematical steps and less computational time. It is also easy to implement, provide closed form expressions [3].

Since the discovery of the high-temperature superconducting materials which have critical temperatures above the boiling point of liquid nitrogen, the development of microwave application of high *T*c superconductors has been extremely rapid and numbers of highly sophisticated subsystem level modules have been generated [6]. High *T*c superconducting microstrip patch antennas have higher gain than their normal counterparts [3], due to the advantages of superconductors [6]. Benefits of using high *T*c superconducting materials at high frequencies include [6]: 1) very small losses, which means low attenuation and low noise level; 2) very low dispersion up to frequencies of several tens of GHz; 3)smaller devices due to minor losses, which leads to greater combination density; and 4) the

transmission phase can be significantly reduced because of the smaller size and shorter interconnects [3], but they suffer from extremely narrow bandwidth, which severely limits their application [3].

Several researchers have studied the resonant characteristics of high-*T*c superconducting microstrip patch antenna [6-8]. To the best of our knowledge, neither any design guideline nor any experimental or theoretical results are available in the open literature to predict the resonant characteristics of high-*T*c superconducting tapered-rectangular microstrip patch realized on anisotropic substances, only results of tapered microstrip antennas printed on unaxial anisotropic substrates have been presented using spectral domain approach [9]. In this chapter, we adjust the cavity method for the analysis of tapered microstri pantenna, in such a way that the method can treat the case of high *T*c superconducting tapered microstrip patch as well as the anisotropic substances. The most important benefit of this approach lies in its mathematical simplicity and low computation time which is more rapidly than the numerical methods and commercially available software.

IV.2. Numerical Results and Discussions

In order to validate the theory presented in the previous chapter, our numerical results are compared with experimental and calculated data previously published [10].

Table IV.1. Comparison of measured and calculated resonant frequency of rectangular microstrip patch for different antennas parameter's, $h_1 = 2.54mm$, $\varepsilon_r = 2.33$.

W (*mm*)	L (*mm*)	Resonant frequencies (GHz)			
		Measured [10]	Simulated HFSS [10]	Calculated [10]	Our results
30	44	2.242	2.223	2.208	2.228
	40	2.47	2.475	2.424	2.446
	36	2.702	2.655	2.686	2.711
	33	2.956	2.985	2.923	2.952
	30	3.184	3.259	3.206	3.239
	24	3.95	4.000	3.978	4.023
	20	4.795	4.712	4.738	4.796
30	30	1.598	1.572	1.603	1.566
	24	1.981	1.956	1.987	1.937
	20	2.3	2.324	2.365	2.299

In Table 1, the resonant frequencies obtained by using the present approach are compared with the measured and calculated resonant frequency of perfectly conductor rectangular patch for different antennas parameter's. The comparison shows that the resonant frequencies computed by the present method are in very good agreement with the measured data for a rectangular patch printed on single substrate.

Table IV.2. Comparison of calculated resonant frequencies with those proposed by Silva et al. [12] and Bedra et al. [6]; $L = 935\,mm$, $W = 1630\,mm$, $t = 350\,nm$, $h = 254\,\mu m$, $T = 50\,K$, $Tc = 89\,K$, $a_0 = 140\,nm$.

Dielectric permittivity (ε_r)	Resonant frequencies (GHz)		
	Full_wave analysis [6]	SDA approach [12]	Our results
11	41.041	41.585	42.573
16	34.856	34.816	35.300
23.81	28.671	28.764	28.937

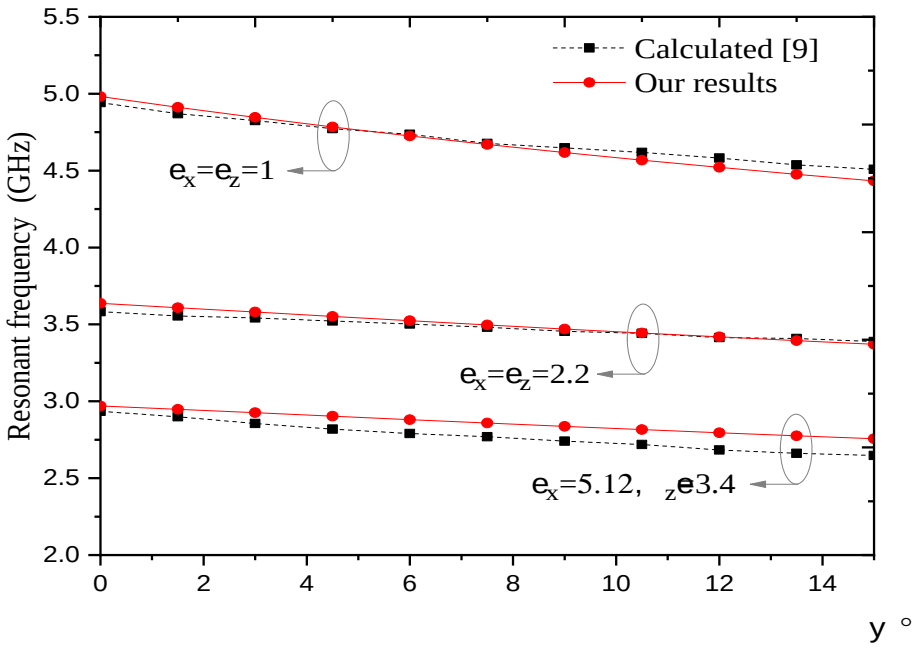

Figure IV.1. Resonant frequency of the dominant mode (TM^{01}) against the inclination angle · for several isotropic/ anisotropic substrates materials; $W = 17.8\,mm$; $L = 26.7\,mm$; $h_1 = 2.54\,mm$.

Table IV. 2 summarizes the calculated resonance frequencies of superconducting rectangular patch and those obtained through the spectral domain approach formulation, for three different dielectric permittivity of the isotropic substrate. Excellent agreement between our

results and those calculated by Full-wave analysis and those obtained by spectral domain approach formulation [6], [12].

Figure IV.1 depicts the variation of the dominant mode of the resonant frequency with the change of the inclination angle. The perfect conductor microstrip patch ($W = 17.8\,mm$, $L = 26.7\,mm$) is printed on several isotropic/anisotropic substrates ($£_x = £_z = 1$; $£_x = £_z = 2.2$; $£_x = 5.12, £_z = 2.2$) with height variation, which means a · variation (Figure 2).

Note that for $· = 0°$ the results are valid for the conventional microstrip antenna. The results of this comparison indicate that the present model shows excellent agreements with those calculated by Silva et all. [12] for all the inclination angle. The computed resonant frequency for various anisotropic substrates is also shown to agree very well with the values computed using SDA approach [6].

The effects of the substrate anisotropy on the resonant frequencies and bandwidths of tapered rectangular patch are shown in Figure IV.3(a) and (b). In these figures, two cases are considered. One is for the case where the substrate is isotropic ($£_x = £_z = 2.2$). The other is for the case of a substrate is anisotropy ($£_x = 5.12, £_z = 2.2$).

Figure IV. 2(a) shows the behavior of the resonant frequency as a function of the thicknesses higher of the perfect conductor tapered antenna. As it is shown in this figure, the resonant frequencies decrease when the thickness h_1, is increased. Also, it can be seen that for a given value of the of the inclination angle ·, the resonant frequency decreases and yields to lower values for the antenna supported by an anisotropic substrate. In Figure IV. 3(b), numerical results are presented for the bandwidth of tapered rectangular patch printed on anisotropic substrate as function of the thickness of the substrate for two different inclination angle · values. In this figure, it is observed that the bandwidth increases with the increase in the thickness substrate, this increase is very clear for higher values of inclination angle · .Also, the use of anisotropic dielectric materials, as antenna substrate, yields to enhancing the bandwidth of the tapered antenna. From all the above observations, it is clear that the material anisotropy has significant effects on the resonant frequency and bandwidth of perfect conductor tapered microstrip antennas.

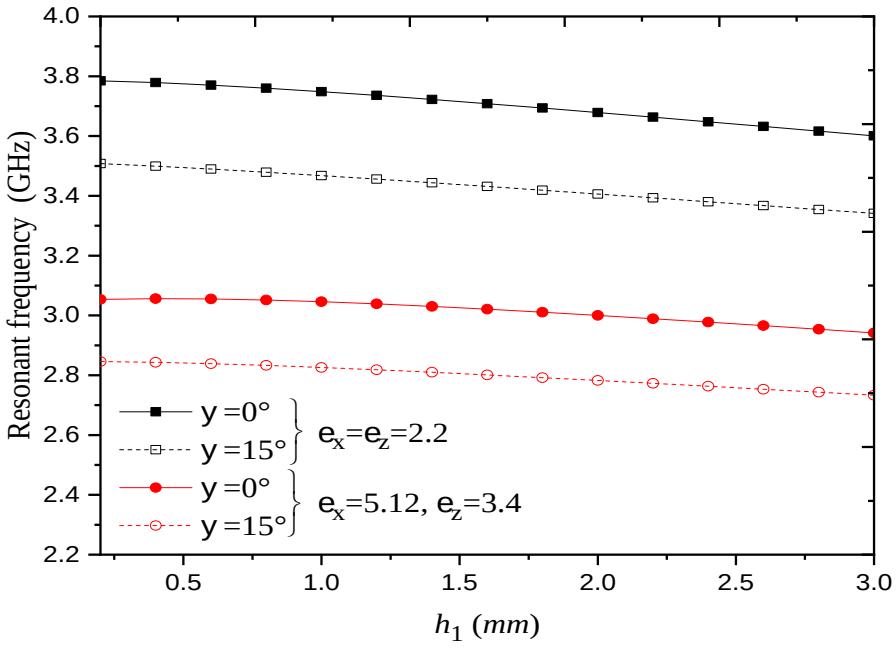

(a)

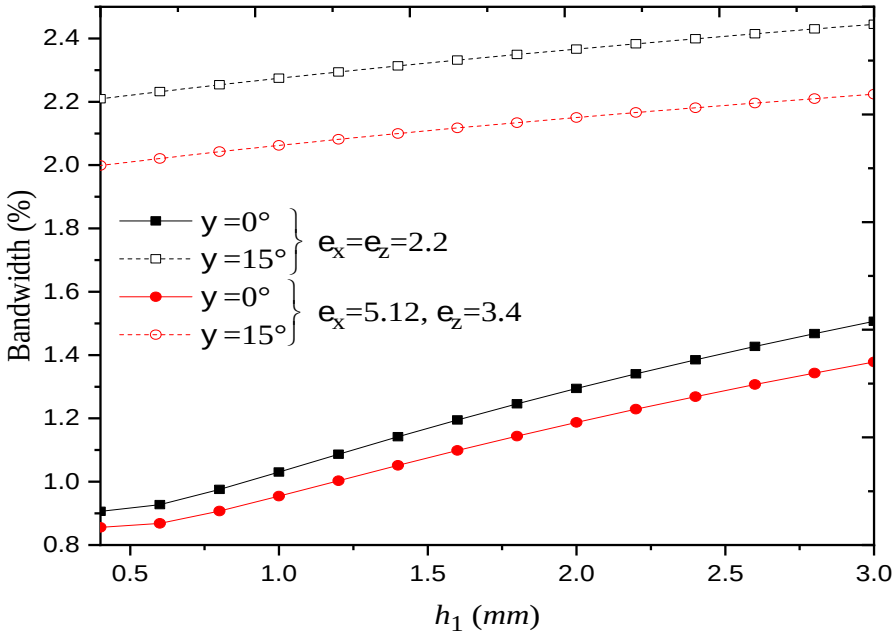

(b)

Figure IV.2. Resonant frequency (a) and bandwidth (b) of tapered microstrip antenna as a function of the thickness of substrates; $W = 17.8\,mm$; $L = 26.7\,mm$; $h_1 = 2.54\,mm$.

In the next step, the influence of the anisotropy on the resonant characteristics of tapered patch antenna is shown in Figure IV.3. The results of the proposed model shown in Figure IV.3 is analyzed using cavity model in conjunction with electromagnetic knowledge approach.

The resonant frequency and bandwidth of the patch antenna against the substrate thickness are shown in Figures IV.3 (a) and (b), where isotropic ($\varepsilon_x = \varepsilon_z = 5.12$), positive uniaxial anisotropic ($\varepsilon_x = 5.12, \varepsilon_z = 6.8$) and negative uniaxial anisotropic ($\varepsilon_x = 5.12, \varepsilon_z = 3.4$) substrates are considered. In Figure IV.3 (a), the anisotropy is obtained by changing ε_z while keeping ε_x constant.

In Figure IV.3 (a), the anisotropy is obtained by changing ε_x while keeping ε_z constant. The effect of the permittivity along the optical axis persists for low as well as for high substrate thicknesses for all values of angle inclination. As for the bandwidth (Figure IV. 3(b)), it is increased due to the negative uniaxial anisotropy and decreased due to the positive uniaxial anisotropy. The resonant frequency and bandwidth of the patch antenna against the substrate thickness are shown in Figures IV.4 (a) and (b), where isotropic ($\varepsilon_x = \varepsilon_z = 3.4$), positive uniaxial anisotropic ($\varepsilon_x = 1.7, \varepsilon_z = 3.4$) and negative uniaxial anisotropic ($\varepsilon_x = 6.8, \varepsilon_z = 3.4$) substrates are considered. The influence of the resonant frequency decreases with reductions in substrate thickness as shown in Figure IV.4 (a). This influence tends to be neglected for lower substrate thickness. These behaviors agree very well with those reported for a various shapes patch antenna, by [13-15].

Figure IV.4 (b) shows the results for the bandwidth of the patch antenna. The positive uniaxial anisotropy slightly increases the bandwidth, while the negative uniaxial anisotropy slightly decreases the bandwidth. The variations of bandwidth due to the uniaxial anisotropy are also seen to increase when the substrate thickness is increased. We can conclude that the permittivity ε_z along the optical axis is the significant and most important factor in determination of the resonant frequency.

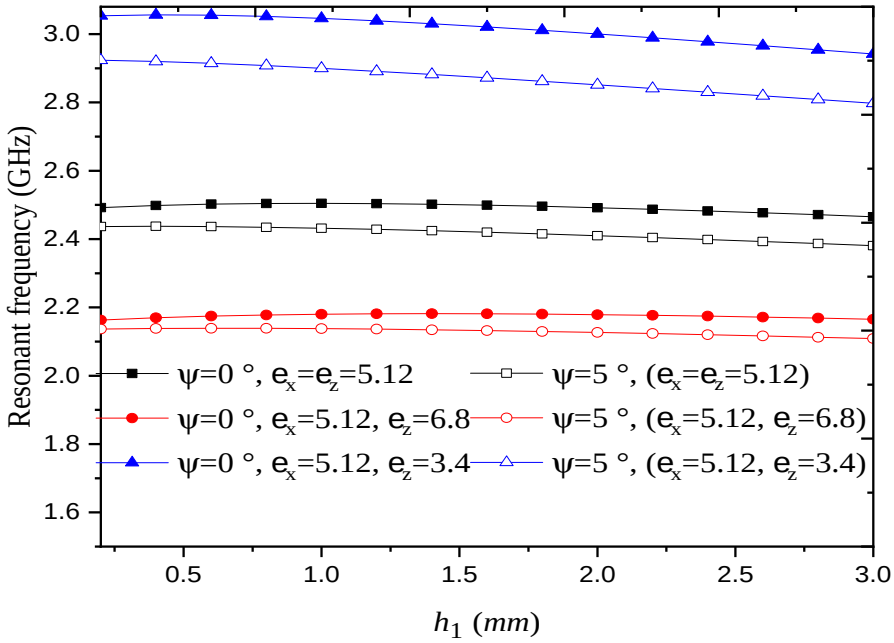

(a)

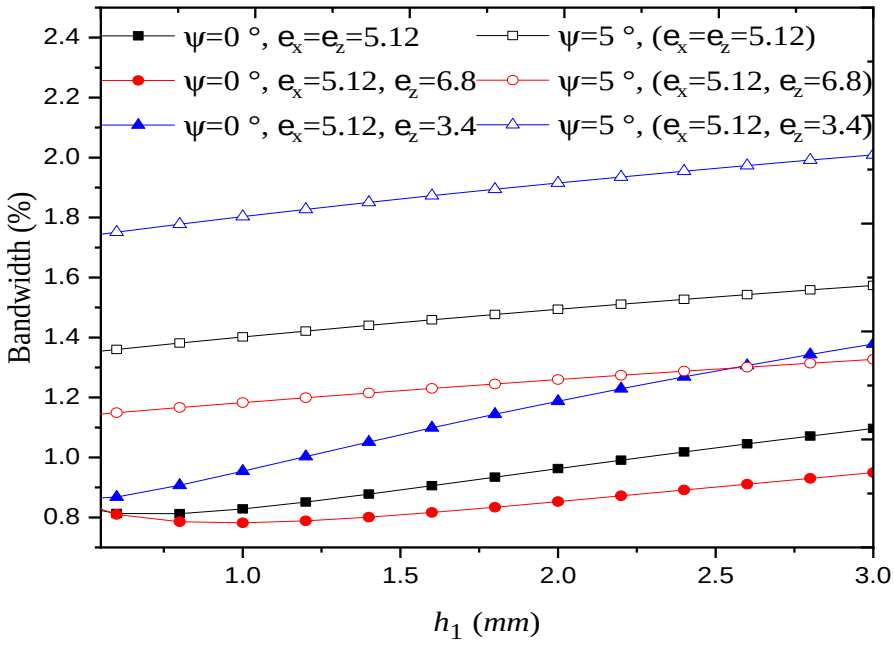

(b)

Figure IV.3. Resonant frequency (a), bandwidth (b) of tapered microstrip antenna versus normalized substrate thicknesses for different permittivity pairs $(\text{£}_x,\text{£}_z)$; $W = 17.8\,mm$, $L = 26.7\,mm$, $h_1 = 2.54\,mm$.

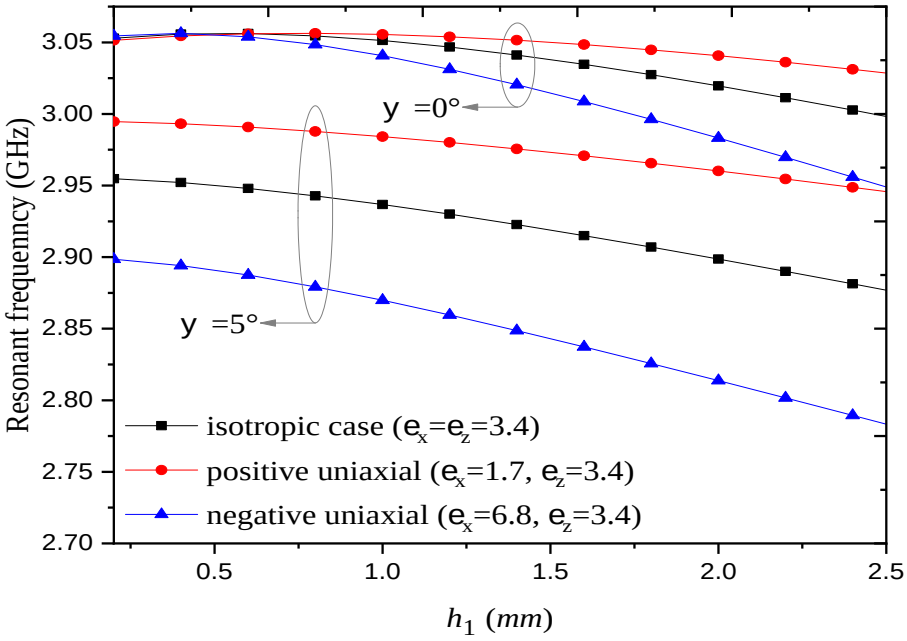

(a)

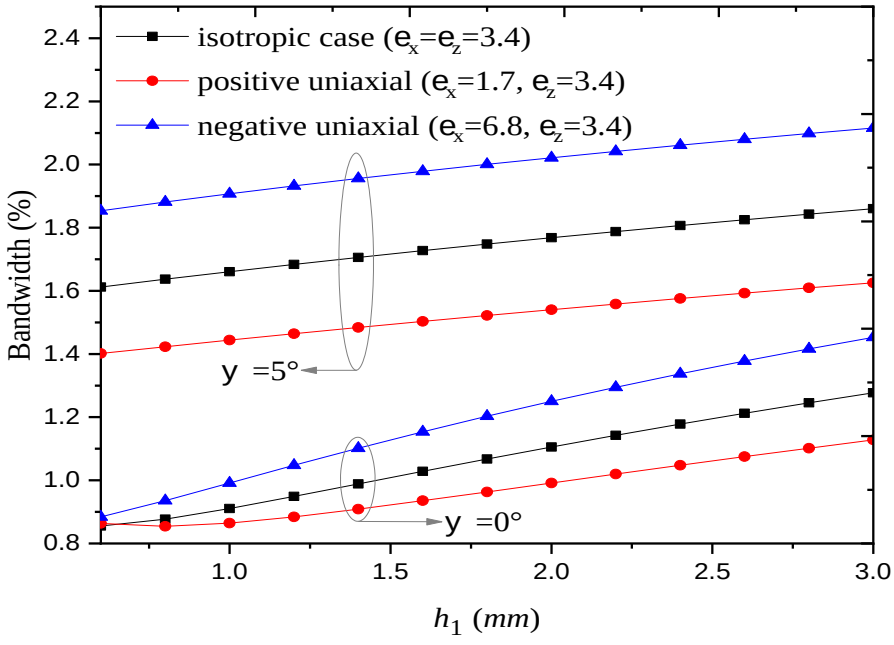

(b)

Figure IV.4. Resonant frequency (a), bandwidth (b) of tapered microstrip antenna versus substrate thicknesses for different permittivity pairs (ε_x,ε_z); $W = 17.8\,mm$, $L = 26.7\,mm$, $h_1 = 2.54\,mm$.

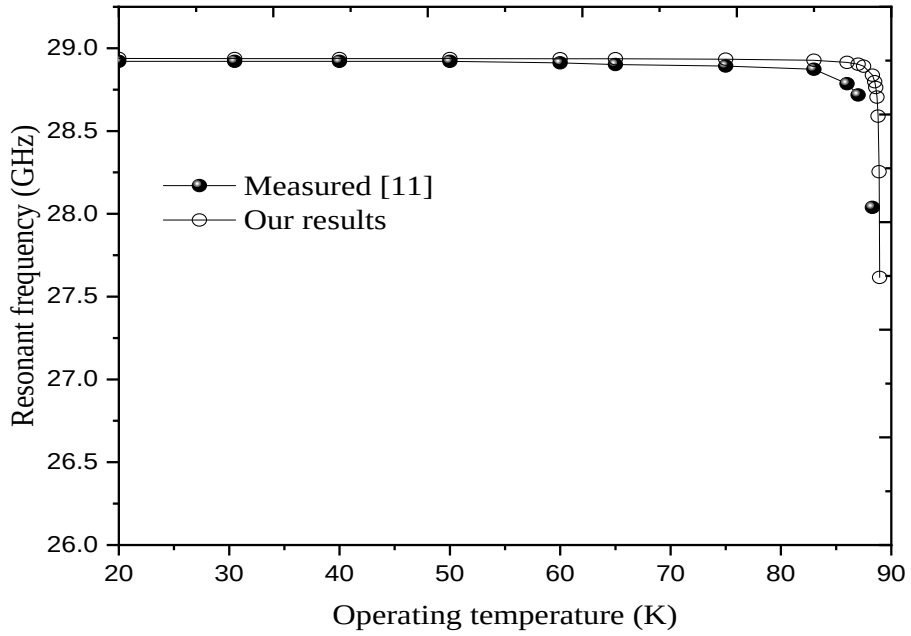

Figure IV.5. Resonant frequency for a tapered microstrip superconducting patch antenna as a function of the operating temperature; $L = 935\ mm$, $W = 1630\ mm$, $t = 350\ nm$, $h = 254\ «m$, $£_r = 23.81$, $Tc = 89\ K$, $ª_0 = 140\ nm$.

To check the present theory for a superconducting rectangular microstrip patch, shown in Figure IV.9, we compared our results with the experimental results of Richard et al. [11]. The rectangular patch of dimension ($L = 935\ mm$, $W = 1630\ mm$), fabricated using a YBCO (YBa2Cu3O7) superconducting thin film of thickness $t = 350\ nm$ with a zero-temperature penetration depth $ª_0 = 140\ nm$ and with a critical temperature $Tc = 89\ K$ .The superconducting patch printed on a lanthanum aluminate substrate (LaAlO3) of thickness $h = 254\ «m$, with permittivity $£_r = 23.81$.

The analysis is carried over the temperature range 20 K to 0.95 *T*c, where *T*c is the transition temperature (*T*c=89 K) of the HTS film. Note that, the variation of the permittivity of the lanthanum aluminate substrate with the change of the temperature, as indicated by the experiment of Richard et al. [11], is taken into account in the present subsection. Results of our modified cavity model show better agreement with the experimental data (see figure IV.5), the error in the resonant frequency (less than 2.5%) is well within the tolerances of the substrate's material parameters.

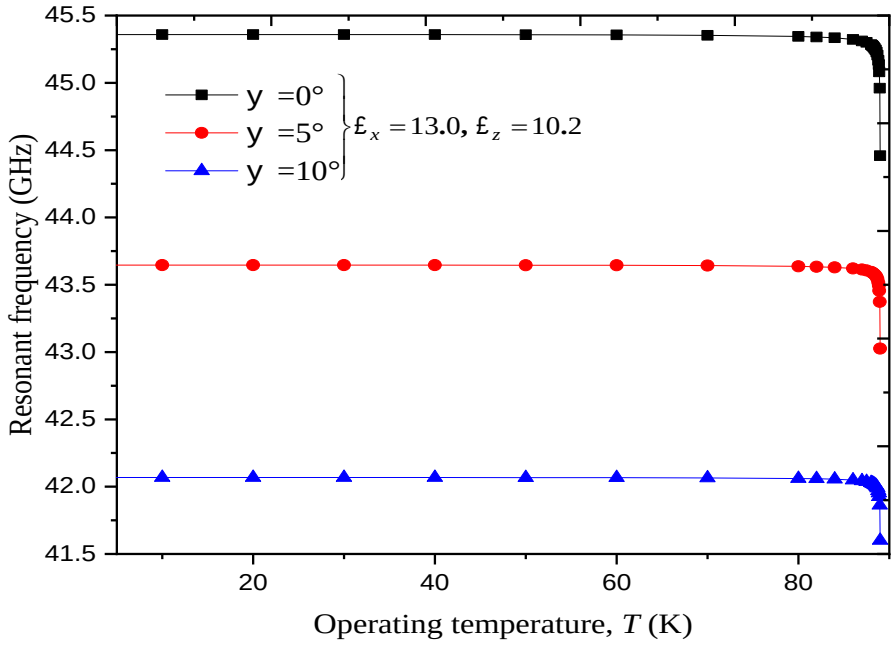

(a)

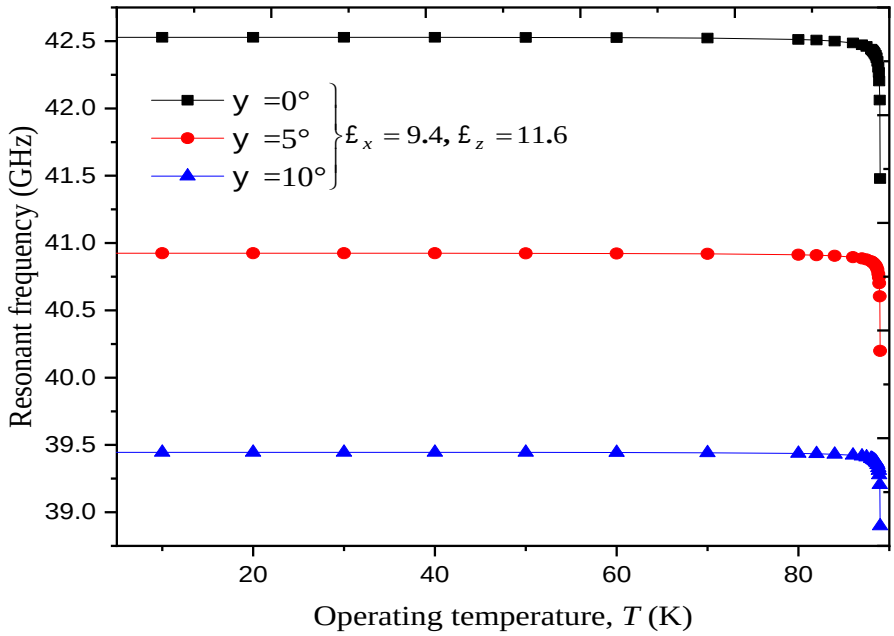

(b)

Figure IV.7. Resonant frequency of the superconducting tapered microstrip patcha gainst operating temperature. The superconducting patch is printed on two different anisotropic substrate materials: $L = 935\ mm$, $W = 1630\ mm$, $t = 280\ nm$, $h = 200\ «m$, $Tc = 89\ K$, $a_0 = 200nm$.

The resonant frequencies of superconducting tapered microstrip antenna as a function of operating temperature for several anisotropic substrates is shown in Figure IV.6. The tapered superconducting film of dimension ($L = 935\ mm$, $W = 1630\ mm$) is of YBCO (YBa2Cu3O7) material characterized by: $t = 280\ nm$, $h = 200\ «m$, $Tc = 89\ K$, $a_0 = 200nm$, printed on Epsilam-10 ($\varepsilon_x = 13$, $\varepsilon_x = 10.2$) anisotropic substrates. From the results of figure IV.6 (a), it can be observed that increasing the temperature will decrease the resonant frequency.

This reduction is significant for temperatures near the transition temperature *T*c. The effects of operating temperature, on the resonant frequency of a high-temperature superconducting tapered patch printed on a Sapphire substrate ($\varepsilon_x = 9.4$, $\varepsilon_x = 11.6$), excited in the dominant mode, is shown in Figures IV.6(b). The variations of the resonant frequency are due to the uniaxial anisotropy substrate decrease gradually with the increase in the temperature. It also observed that the resonant frequencies obtained when the inclination angle= 0° are higher than those obtained when the inclination angle =5° and the inclination angle=10°.

This reduction becomes more significant for the values of temperature close to the critical temperature (*T*c). These behaviors agree very well with those reported elsewhere in [15]. Note that the abrupt change in the resonant frequency at temperatures near *T*c can be attributed to a modification of the magnetic penetration depth of the YBCO [11]. It also observed that the resonant frequencies obtained when the superconducting patch is printed on Epsilam-10 ($\varepsilon_x = 13$, $\varepsilon_x = 10.2$) are higher than those obtained when the superconducting patch is printed on the Sapphire substrate ($\varepsilon_x = 9.4$, $\varepsilon_x = 11.6$) because the effective relative permittivity of the Epsilam-10 is lower than the one of the Sapphire material.

Figures IV.7 illustrate the variation of the resonant frequency of the superconducting tapered microstrip patch against thickness of superconducting patch. The superconducting patch is printed on two different anisotropic substrate materials using the same anisotropic substrates using in figure IV.6. It can be seen that as the thickness of superconductor patch grows, the resonant frequency increases quickly until the thickness (*t*) reaches $a_0 = 200nm$ (penetration depth). After this value, increasing the superconducting thickness will increase slowly the resonance frequency.

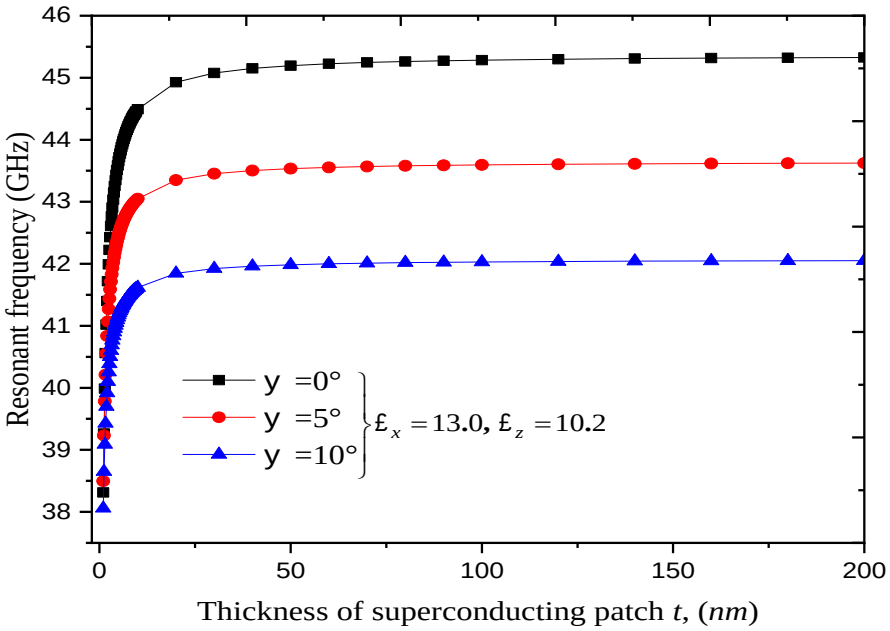

(a)

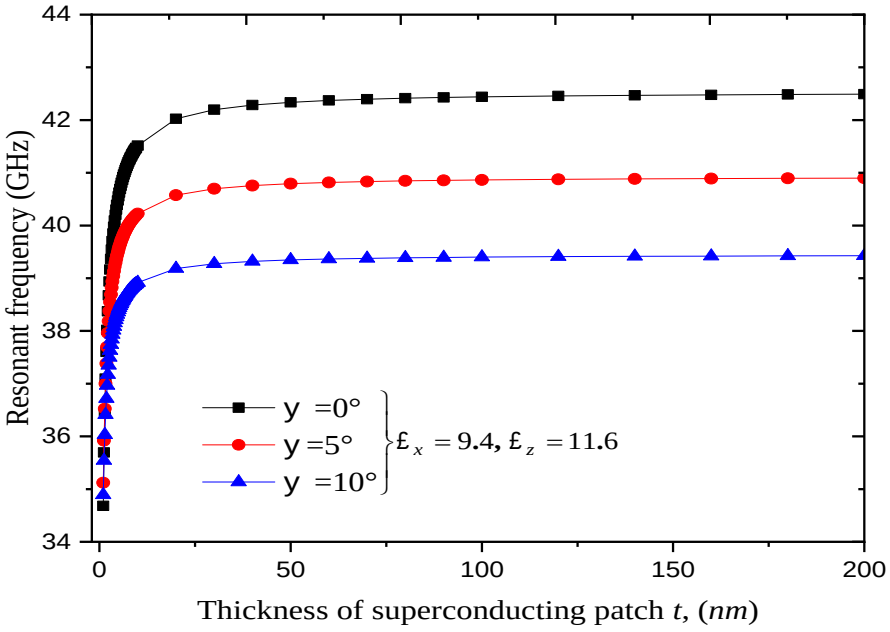

(b)

Figure IV.7. Resonant frequency of the superconducting tapered microstrip patch against thickness of superconducting patch. The superconducting patch is printed on two different anisotropic substrate materials: $L = 935\ mm$, $W = 1630\ mm$, $h = 200\ «m$, $T = 75\ K$, $Tc = 89\ K$, $a_0 = 200nm$.

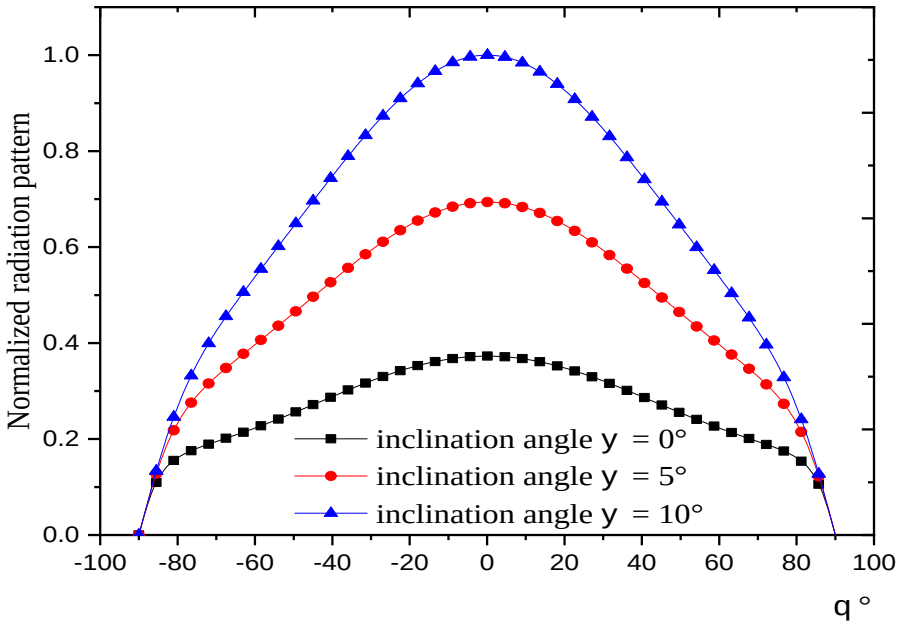

(a)

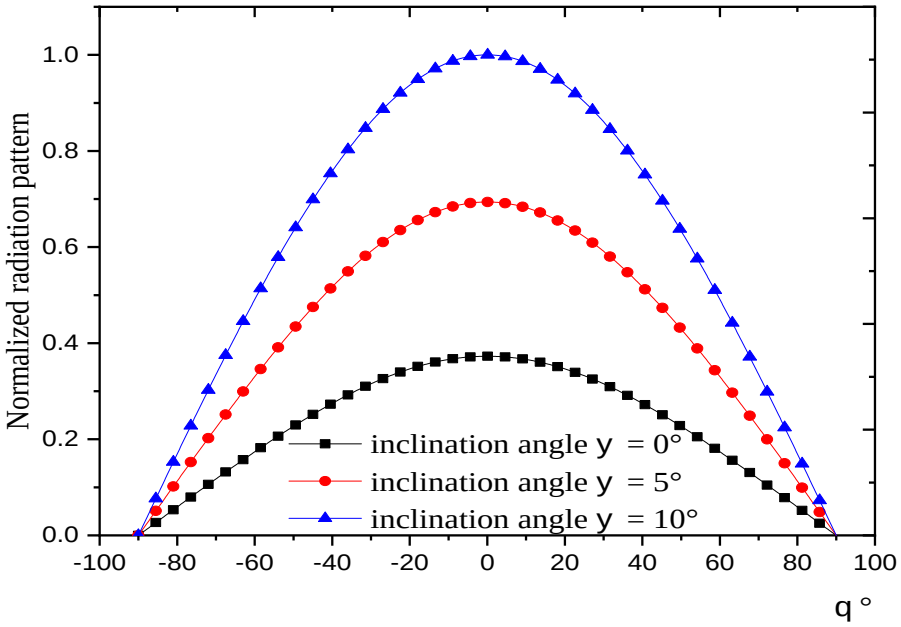

(b)

Figure IV.8. Normalized radiation pattern of the of perfect conductor tapered patch printed on isotropic substrate, (a) E-plane, (b) H-plane; $W = 17.8\,mm$; $L = 26.7\,mm$; $h = 254\,«m$, $£_r = 2.2$.

FigureIV.8 illustrate the variation of the Normalized radiation pattern of the of perfect conductor tapered patch printed on isotropic substrate, with the change of the inclination angle, for the two principal plans, (a) E-plane, (b) H-plane. It observed that the antenna directivity obtained when the inclination angle= 10° are higher than those obtained when the inclination angle=5°and the inclination angle=0°. The result shows that directivity of the antenna increases with decreasing in the inclination angle.

Figure IV.9 shows the normalized radiation patterns of tapered HTS structure printed on two different anisotropic substrates: Epsilam-10 ($£_x = 13, £_x = 10.2$) and Sapphire ($£_x = 9.4$, $£_x = 11.6$), with the antenna parameters are : $L = 1100\ mm$, $W = 1700\ mm$, $h = 200\ «m$, $T = 77\ K, Tc = 86\ K$, $ª_0 = 180\ nm$, $t = 350\ nm$.

In Figure IV.9 (a), we plot the variation on the normalized radiation pattern in the E-plane, for two anisotropic materials, while in Figure IV.9 (b), we plot the variation on the normalized radiation patterns in H-plane. The two cases of the substrates are illustrated. From these results, it is seen that the E-plane radiation is sensitive to the variation of the substrate materials. Note that the directivity of the antenna with Sapphire ($£_x = 9.4$, $£_x = 11.6$) is lower than the one with Epsilam-10 ($£_x = 13, £_x = 10.2$).

The results show that the directivity patterns of superconducting microstrip antenna increases as the effective permittivity of the substrate decreases. This result agrees with that discovered theoretically for superconducting rectangular microstrip patches [6].

The coefficient reflection (S^{11}) of tapered microstrip antenna was simulated at frequencies over 1.5–3.0 GHz range using HFSS ™ simulator. Figure IV.11 shows the (S^{11}) curve of tapered microstrip antenna for several inclination angle · . The antenna parameters are: $W = 17.8\ mm$; $L = 26.7\ mm$; $h = 2.54\ mm$. We observed that the resonant frequencies are shifted to 2.45 and 2.31 GHz, respectively. From this figure, it can be observed that the tapered microstrip antenna with inclination angle at 0.14 GHz lower frequency than the tapered microstrip antenna without inclination angle.

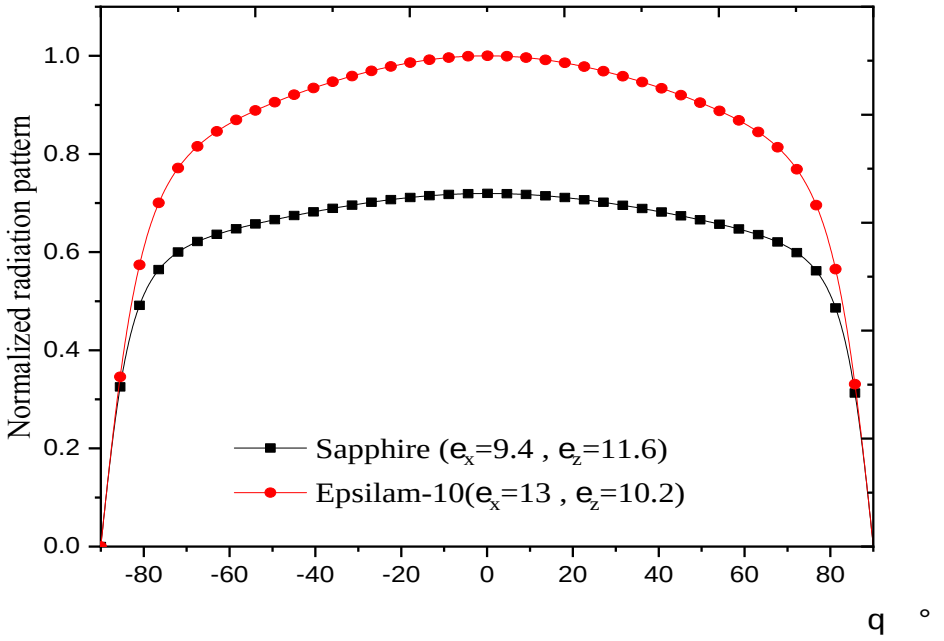

(a)

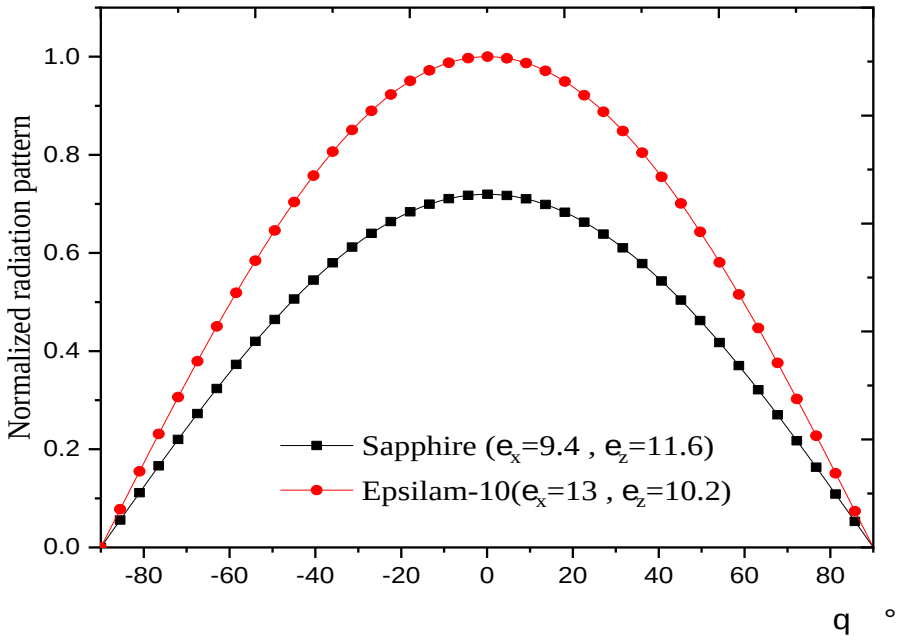

(b)

Figure IV.9. Normalized radiation pattern of the of superconducting tapered patch printed on isotropic substrate, (a) E-plane, (b) H-plane; $L = 1100\ mm$, $W = 1700\ mm$, $h = 200\ «m$, $T = 77\ K$, $Tc = 86\ K$, $a_0 = 180\ nm$, $t = 350\ nm$.

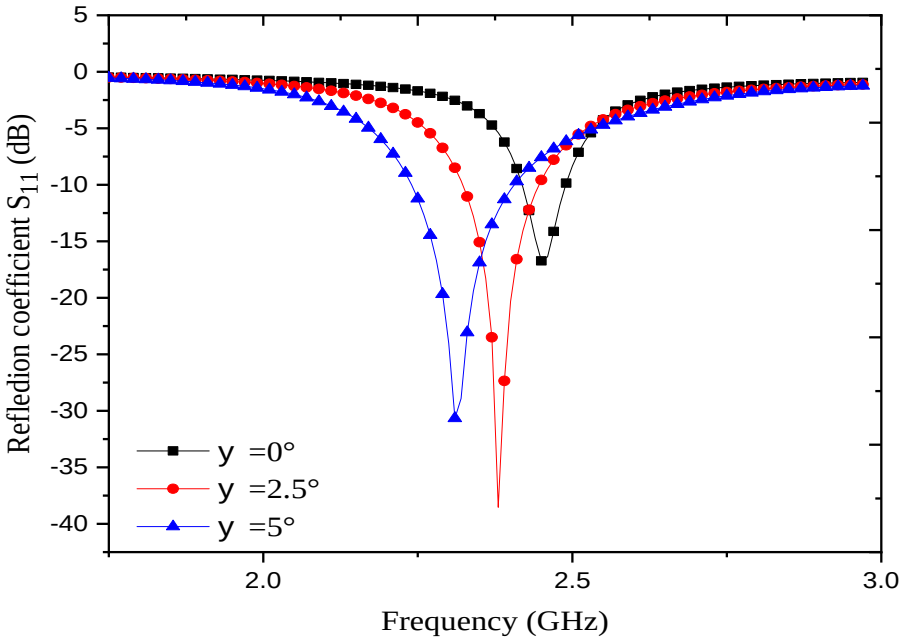

Figure IV. 10. Return loss S_{11} curve of the antenna as function of operating frequencies, for several inclination angle, (b) H-plane; $W = 17.8\,mm$, $L = 26.7\,mm$, $h = 2.54\,mm$, $£_x = £_z = £_r = 3.4$.

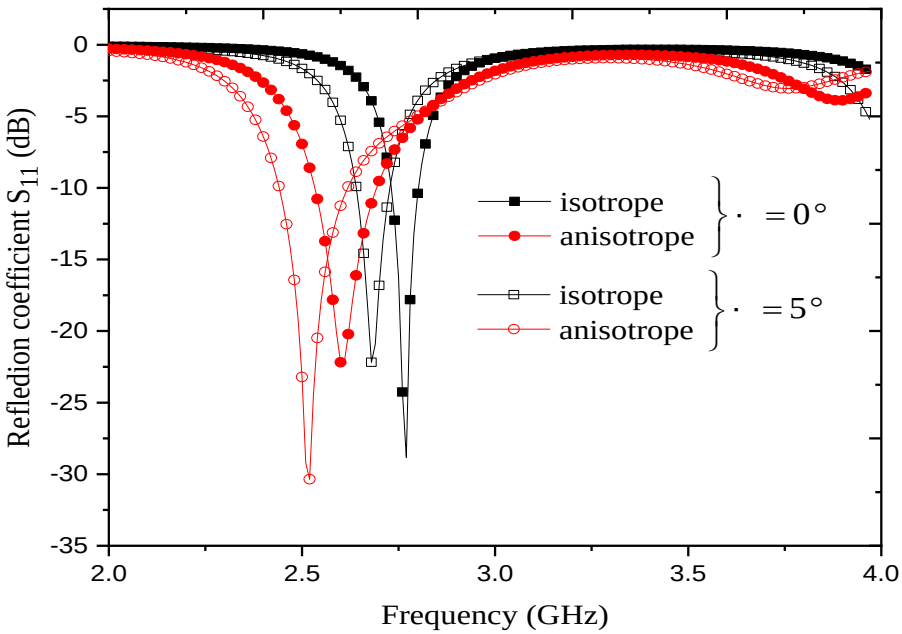

Figure IV. 11. Return loss S_{11} curve of the antenna as function of operating frequencies, for several inclination angle considering and neglecting anisotropic substrate; $W = 17.8\,mm$, $L = 26.7\,mm$, $h = 2.54\,mm$, isotropic case ($£_x = £_z = £_r = 3.4$), anisotropic case ($£_x = 3.4,\ £_z = 5.12$).

Figure IV.11 present the variation of the return loss S^{11} as function of the operating frequency of tapered microstrip antenna printed on isotropic / anisotropic substrates.

The simulated relative -10dB impedance bandwidth of the tapered antenna for the isotropic case is 2.89% without inclination angle $\cdot = 0°$, and 3.73 % when inclination angle is considered $\cdot = 5°$. Note that the for the case of anisotropic substrate, the simulated relative -10dB impedance bandwidth of the tapered microstrip antenna rich than 6.51 % without inclination angle $\cdot = 0°$, and 7.14 % when inclination angle is considered $\cdot = 5°$. Hence, the bandwidth improvement using the anisotropic substrate has been well demonstrated.

IV.3. Conclusion

In this chapter, an efficient approach based on cavity model in conjunction with electromagnetic knowledge has been described for computation of resonant frequencies and bandwidths of an HTS tapered microstrip patch antenna printed on isotropic / anisotropic substrates. The resonant frequencies and bandwidths calculated by using the present technique have been compared with those previously measured and calculated results available in the various literatures, and excellent consistency has been found. It is shown that the effect of high *T*c superconducting film becomes more significant for the values of temperature close to the critical temperature. Also, it is shown that uniaxially anisotropic substrate affects the resonant characteristics of the superconducting microstrip antenna and consequently they must be taken into account in the design stage. Our proposed model can be extended to a tapered microstrip patch in an anisotropic ferrite multilayer environment. This model, however, gives a quite good approximation of the superconducting antenna's behavior and leads to a very short calculation time for the analysis.

IV.4. References

[1] R. Bedra, "Etude d'une antenne supraconductrice couverte par une couche diélectrique," *Thèse de Doctorat, Université de Batna 2*, Algérie, 2018.

[2] S. Bedra, R. Bedra, S. Benkouda, and T. Fortaki, "Superstrate loading effects on the resonant characteristics of high Tc superconducting circular patch printed on anisotropic materials," *Physica C: Superconductivity and Its Applications*, vol. 543, pp. 1-7, 2017.

[3] S. Bedra, R. Bedra, S. Benkouda, and T. Fortaki, "Efficient CAD Model to Analysis of High Tc Superconducting Circular Microstrip Antenna on Anisotropic Substrates," *Advanced Electromagnetics*, vol. 6, no. 2, pp. 40-45, 2017.

[4] A. S. Boughrara, S. Benkouda, A. Bouraiou, and T. Fortaki, "Study of Stacked High Tc Superconducting Circular Disk Microstrip Antenna in Multilayered Substrate Containing Isotropic and/or Uniaxial Anisotropic Materials," *Advanced Electromagnetics*, vol. 8, no. 3, pp. 1-5, 2019.

[5] A. Mahamdi, S. Benkouda, S. Aris, and T. A. Denidni, "Resonant Frequency and Bandwidth of Superconducting Microstrip Antenna Fed through a Slot Cut into the Ground Plane," *Electronics*, vol. 10, no. 2, p. 147, 2021.

[6] S. Bedra and T. Fortaki, "Effects of superstrate layer on the resonant characteristics of superconducting rectangular microstrip patch antenna," *Progress In Electromagnetics Research C*, vol. 62, pp. 157-165, 2016.

[7] O. Barkat, "Modeling and optimization of radiation characteristics of triangular superconducting microstrip antenna array," *Journal of Computational Electronics*, vol. 13, no. 3, pp. 657-665, 2014.

[8] M. Lamine Tounsi and M. C. E. Yagoub, "Efficient characterization of EMC shielding in anisotropic high- Tc superconducting devices for industrial applications," *International Journal of RF and Microwave Computer- Aided Engineering*, vol. 22, no. 1, pp. 116-123, 2012.

[9] M. Albuquerque, A. G. d'Assuncao, and S. G. da Silva, "Broadband microstrip patch antennas on anisotropic substrates," lntemational Conference on Antennas and Propagation, IEE, vol. 1, pp. 49-52. 2001.

[10] M. Biswas and M. Sen, "Fast and accurate model for a coax-fed rectangular patch antenna with varying aspect ratio, feed location and substrate electrical parameters," *Journal of Electromagnetic Waves and Applications*, vol. 33, no. 4, pp. 428-453, 2019.

[11] M. A. Richard, K. B. Bhasin, and P. C. Claspy, "Superconducting microstrip antennas: an experimental comparison of two feeding methods," *IEEE Transactions on Antennas and Propagation*, vol. 41, no. 7, pp. 967-974, 1993.

[12] S.G. da Silva, A.G. d'Assunção, J.R.S. Oliveira, Analysis of high Tc superconducting microstrip antennas and arrays, IEEE (1999) 243–246, 1999.

[13] M. L. Bouknia *et al.*, "Analysis of the combinatory effect of uniaxial electrical and magnetic anisotropy on the input impedance and mutual coupling of a printed dipole antenna," *IEEE Access*, vol. 9, pp. 84910-84921, 2021.

[14] M. L. Bouknia *et al.*, "Effect analysis of the general complex reciprocal gyro-bianisotropic metamaterial medium on the input impedance of a printed dipole antenna," *Alexandria Engineering Journal*, vol. 61, no. 5, pp. 3691-3696, 2022.

[15] S. Bedra, S. Benkouda, R. Bedra, and T. Fortaki, "Inverted HTS rectangular patch antennas: Theoretical investigation," *Physica C: Superconductivity and its Applications*, vol. 580, p. 1353802, 2021.

General Conclusion

General conclusion

Nowadays, patch antenna has known as one of the most important elements in wireless communication system. It is use as radiating and receiving element in wide range of microwaves system such as radar, remote sensing, communication and radio frequency. By the early 21st century, the evolution of antennas became rapid [1].

In this work, we started with a brief presentation of some general information on microstrip antennas. Thereafter we detailed the principle of operation, the advantages, and the limitations of the various techniques used to feed these antennas. The presentation of the different applications of these types of antennas is also discussed. We have demonstrated the possibility of adopting analytical modeling for rectangular and tapered patch antennas. For this, we based ourselves on the modified cavity model. This approach takes into account the physical properties of the geometric parameters of the tapered patch antenna. We have tried to enrich the CAD heritage of plated microstrip resonators through the application of the modified cavity method to new structures and to give more relevant explanations of the physical phenomena governing the behavior of these resonators, our results have been compared and are considered very satisfactory [2].

The results obtained show that: The increase in temperature causes a decrease in the resonant frequency. This decrease is significant for temperature values close to the critical temperature. The resonant frequency is related to the physical parameters of the antenna (thickness of the substrate, length of the patch, dielectric constant). The results concerning the resonant frequency as a function of the thickness of the superconducting patch show that the resonant frequency increases with the increase in the thickness of the patch.

We also noticed that the effect of superconductivity thickness on resonance frequency and bandwidth is more pronounced for values less than half the value of zero-temperature penetration depth. Also, the dielectric anisotropy of the substrate can introduce severe degradation of the scanning characteristics if the anisotropic effects are neglected. Therefore, a considerable improvement of the superconducting antenna bandwidth is obtained by a choice choose of the anisotropic substrate.

The work presented in this work has shown that the use of a superconducting patch offers additional degrees of freedom in the design of these antennas, so, we can to continue research in this area, but using structures more complex involving several patches and anisotropic substrates of electric and magnetic type [3].

I References

[1] M. N., HUSIN, JUSOH, M. T., and DIN, M. F. M., ''Study and design of U-shaped patch antenna for multiband application,'' *Joural of Fundamental and Applied Sciences*, vol. 9, no 3S, p. 578-589, 2017.

[2] T.Karim and S.M .seddik, '' Modèle de cavité amélioré d'un résonateur microbande réglable pour ele l'application dans un équipement portable sans fil,'' mémoire de master, université Abbes laghrour, khenchela , 2021.

[3] L, M. Lamine, and A, Yassine, ''Analyse d'une antenne microbande à secteur supraconducteur circulaire ele imprimé sur des substrats suspendus et composites,'' mémoire de master, université de Khenchela, 2020.

الملخص

الهدف من هذا العمل هو تحليل هوائيات microstrip المستطيلة باستخدام نموذج التجويف بالاشتراك مع المعرفة الكهرومغناطيسية. نقوم بتوسيع التحليل النظري المقدم بحيث يكون صالحًا لدراسة بقع مستطيلة فائقة التوصيل مدببة مطبوعة على مواد كهربائية غير متباينة الخواص / أو متباينة الخواص. لقد اخترنا هذه الطريقة لأنها، على عكس الأساليب الصارمة، توفر فهمًا نوعيًا ولا تتطلب تعقيدات رياضية، لأنها تتضمن خطوات رياضية، ووقتًا حسابيًا أقل، وأسهل في التحليل. تم إجراء دراسة شاملة لتحديد تأثير المعلمات الكهربائية والفيزيائية على أداء الهوائي مع مراعاة تباين الخواص العازلة تمت مقارنة النتائج العددية لهوائي HTS المدبب مع البيانات النظرية والتجريبية الواردة في الأدبيات. يعتبر التصميم النظري هذا مفيدًا جدًا للتنفيذ العملي لهوائيات microstrip في المعدات اللاسلكية المحمولة.

الكلمات المفتاحية- هوائيات Microstrip مدببة ؛ النمذجة والتصميم؛ تردد الرنين ؛ ركائز متباينة الخواص ؛ الاتصالات اللاسلكية.

Résumé

L'objectif principal de ce travail est d'étudier les antennes microruban rectangulaires en utilisant le modèle de cavité conjointement avec les connaissances électromagnétiques. Nous étendons l'analyse théorique présentée afin qu'elle soit valable pour l'étude de patchs supraconducteurs effilés rectangulaires imprimés sur des matériaux diélectriques isotropes et/ou anisotropes. Nous avons choisi cette méthode car, contrairement aux méthodes rigoureuses, elle fournit une compréhension qualitative et ne nécessite pas de complexités mathématiques, elle implique des étapes mathématiques, moins de temps de calcul et est plus facile à analyser. Une étude approfondie a été menée pour déterminer l'effet des paramètres électriques et physiques sur les performances de l'antenne, en tenant compte de la variance des propriétés diélectriques. Les résultats numériques de l'antenne effilée HTS sont comparés aux données théoriques et expérimentales rapportées dans la littérature. Cette conception théorique est très utile pour la mise en œuvre pratique des antennes microruban dans les équipements sans fil portables.

***Mots Clés**- Antennes Microbandes Effilées ; Modélisation & Conception ; Fréquence de résonance ; Substrats Anisotropes ; communications sans fil.*

Abstract

The main objective of this work is to study rectangular microstrip antennas using the cavity model in combination with electromagnetic knowledge. We extend the presented theoretical analysis so that it is valid for studying rectangular tapered superconducting patches printed on isotropic and/or anisotropic dielectric materials. We chose this method because, unlike rigorous methods, it provides qualitative understanding and does not require mathematical complexities, because it involves mathematical steps, less computational time, and is easier to analyze. A comprehensive study was conducted to determine the effect of electrical and physical parameters on antenna performance, taking into account the variance of dielectric properties. The numerical results of the HTS tapered antenna are compared with the theoretical and experimental data reported in the literature. This theoretical design is very useful for the practical implementation of microstrip antennas in portable wireless equipment.

Keywords *– Tapered Microstrip Antennas; Modeling & Design; Resonant frequency; Anisotropic substrates; wireless communications.*